THE JOURNAL OF BIOLOGICAL CHEMISTRY VOL. 291, NO. 1, pp. 318–333, January 1, 2016

Proteolytic Processing of Neuregulin 1 Type III by Three Intramembrane-cleaving Proteases

Received for publication, October 19, 2015, and in revised form, November 3, 2015 Published, JBC Papers in Press, November 16, 2015, DOI 10.1074/jbc.M115.697995

Daniel Fleck[‡1,2], Matthias Voss[‡1,3], Ben Brankatschk[§], Camilla Giudici[‡], Heike Hampel[‡], Benjamin Schwenk[¶], Dieter Edbauer[¶‖], Akio Fukumori[¶], Harald Steiner[‡¶], Elisabeth Kremmer[‖], Martina Haug-Kröper[‡], Moritz J. Rossner[§], Regina Fluhrer[‡¶], Michael Willem[‡4], and Christian Haass[‡¶‖5]**

*From the [‡]Biomedical Center, Biochemistry, Ludwig-Maximilians-University Munich, 81377 Munich, the [§]Department of Molecular Neurobiology, Clinic for Psychiatry, Ludwig-Maximilians-University Munich, 80336 Munich, the [¶]German Center for Neurodegenerative Diseases (DZNE), Munich, 81377 Munich, the [‖]Munich Cluster for Systems Neurology (SyNergy), 81377 Munich, and the **Institute of Molecular Immunology, Helmholtz Center Munich, 81377 Munich, Germany*

Numerous membrane-bound proteins undergo regulated intramembrane proteolysis. Regulated intramembrane proteolysis is initiated by shedding, and the remaining stubs are further processed by intramembrane-cleaving proteases (I-CLiPs). Neuregulin 1 type III (NRG1 type III) is a major physiological substrate of β-secretase (β-site amyloid precursor protein-cleaving enzyme 1 (BACE1)). BACE1-mediated cleavage is required to allow signaling of NRG1 type III. Because of the hairpin nature of NRG1 type III, two membrane-bound stubs with a type 1 and a type 2 orientation are generated by proteolytic processing. We demonstrate that these stubs are substrates for three I-CLiPs. The type 1-oriented stub is further cleaved by γ-secretase at an ε-like site five amino acids N-terminal to the C-terminal membrane anchor and at a γ-like site in the middle of the transmembrane domain. The ε-cleavage site is only one amino acid N-terminal to a Val/Leu substitution associated with schizophrenia. The mutation reduces generation of the NRG1 type III β-peptide as well as reverses signaling. Moreover, it affects the cleavage precision of γ-secretase at the γ-site similar to certain Alzheimer disease-associated mutations within the amyloid precursor protein. The type 2-oriented membrane-retained stub of NRG1 type III is further processed by signal peptide peptidase-like proteases SPPL2a and SPPL2b. Expression of catalytically inactive aspartate mutations as well as treatment with 2,2′-(2-oxo-1,3-propanediyl)bis[(phenylmethoxy)carbonyl]-L-leucyl-L-leucinamide ketone inhibits formation of N-terminal intracellular domains and the corresponding secreted C-peptide. Thus, NRG1 type III is the first protein substrate that is not only cleaved by multiple sheddases but is also processed by three different I-CLiPs.

Regulated intramembrane proteolysis typically involves an initial shedding of a membrane-bound protein followed by intramembrane cleavage of the remaining membrane-tethered stub via intramembrane-cleaving proteases (I-CLiPs)[6] (1–3). All I-CLiPs are polytopic proteases with their catalytic domains embedded within transmembrane domains (TMDs) (2). Intramembrane-cleaving metallo-, serine-, aspartyl-, and glutamyl-proteases have so far been identified. The aspartyl-proteases belong to the G*X*GD-type proteases, where G*X*GD describes the consensus sequence around the N-terminal critical aspartyl residue (4, 5). The founding members of this I-CLiP family are the presenilins (PS1 and PS2), the catalytically active subunit of the γ-secretase complex (4, 5). Besides PS, Aph1a/b, nicastrin, and Pen-2 are critically required for γ-secretase assembly and activity (6, 7). Intramembrane proteolysis by γ-secretase occurs via multiple cleavages starting at an ε-site close to the C-terminal end of the TMD and ending after an intermediate cut at a ζ-site at the γ-site in the middle of the TMD (8–10). γ-Secretase processes numerous membrane-retained type 1-oriented C-terminal stubs (11). γ-Secretase cleavage liberates intracellular domains (ICD), which can be involved in reverse signaling as well as small secreted peptides such as amyloid β-peptide (Aβ) (6). However, in many cases γ-secretase processing may contribute to the final degradation of membrane fragments (12). Whereas γ-secretase exclusively accepts type 1 substrates, type 2-oriented membrane fragments are cleaved by I-CLiPs belonging to the signal peptide peptidase (SPP) and SPP-like (SPPL) subfamily of mammalian G*X*GD

* This work was supported in part by Deutsche Forschungsgemeinschaft Grants HA 1737-11, FL 635/2-1, FOR2290, and HA 1737/13-1 and a MetLife Award. The authors declare that they have no conflicts of interest with the contents of this article.

[1] Recipient of Ph.D. stipends from the Hans and Ilse Breuer Foundation.
[2] Present address: Genentech, 1 DNA Way, South San Francisco, CA 94080.
[3] Present address: Center for Infectious Medicine, Dept. of Medicine, Karolinska Institute, Karolinska University Hospital Huddinge, 141 86 Stockholm, Sweden.
[4] To whom correspondence may be addressed: Institute for Metabolic Biochemistry, Ludwig-Maximilians-University and the German Center for Neurodegenerative Diseases (DZNE), Feodor-Lynen Strasse 17, 81377 Munich, Germany. Tel.: 89-4400-46549; E-mail: Michael.Willem@mail03.med.uni-muenchen.de.
[5] To whom correspondence may be addressed: Institute for Metabolic Biochemistry, Ludwig-Maximilians-University, and the German Center for Neurodegenerative Diseases (DZNE), Feodor-Lynen Strasse 17, 81377 Munich, Germany. Tel.: 89-4400-46549; E-mail: christian.haass@mail03.med.uni-muenchen.de.

[6] The abbreviations used are: I-CLiP, intramembrane-cleaving protease; ADAM, a disintegrin and metalloprotease; Aβ; amyloid β-peptide; APP, β-amyloid precursor protein; BACE1, β-site APP-cleaving enzyme 1; CTF, C-terminal fragment; ICD, intracellular domain; NRG1, neuregulin 1; NTF, N-terminal fragment; PS, presenilin; SPP, signal peptide peptidase; SPPL, SPP-like; SNP, single nucleotide polymorphism; TMD, transmembrane domain; Tricine, *N*-[2-hydroxy-1,1-bis(hydroxymethyl)ethyl]glycine; GV, Gal4-VP16; IP, immunoprecipitation; $(Z\text{-}LL)_2$, 2,2′-(2-oxo-1,3-propanediyl)-bis[(phenylmethoxy)carbonyl]-L-leucyl-L-leucinamide; DAPT, *N*-[*N*-(3,5-difluorophenacetyl)-L-alanyl]-*S*-phenylglycine *t*-butyl ester; IAA, iodoacetic acid.

proteases (13). SPP/SPPLs share structural features with PSs, including the characteristic overall topology and the essential catalytic G*X*GD motif (14). SPP cleaves endoplasmic reticulum-resident substrates, which include, among others, signal peptides (14) and tail-anchored endoplasmic reticulum proteins (15). At least SPP and SPPL2b cleave type 2 membrane protein stubs following shedding (13, 16, 17). Similar to some γ-secretase substrates, ICDs liberated from their membrane anchors by SPPL2a/SPPL2b have been reported to regulate gene expression (17, 18). For SPPL3, a rather unexpected and exceptional function has been shown very recently. SPPL3 sheds glycosyltransferases and thereby regulates their intracellular activity (19).

Sheddases comprise proteases of the ADAM (A Disintegrin And Metalloproteinase) and BACE (β-site APP cleaving protease) family as well as several other mostly membrane-bound proteases. BACE1 and ADAM10 as well as ADAM17 play pivotal roles in proteolytic processing of the β-amyloid precursor protein (APP). Whereas BACE1 generates the N terminus of Aβ, ADAM10 and ADAM17 prevent amyloidogenesis by cleaving within the Aβ domain (6). However, sheddases have numerous substrates. For example, for BACE1 more than 30 different brain-specific substrates have been identified (20, 21), among them neuregulin 1 type III (NRG1 type III) (22, 23). Shedding of NRG1 type III is initiated by BACE1 or ADAM10/17 (Fig. 1*A*). This cleavage exposes the epidermal growth factor (EGF)-like domain to allow ErbB3 signaling, which is required for myelination of the peripheral nervous system during early postnatal development. Consequently, a BACE1 knock-out in mice and zebrafish selectively reduces myelination of the peripheral nervous system (22, 24). In contrast to the processing of NRG1 type I, shedding of the hairpin-structured NRG1 type III not only generates a type 1- but additionally a type 2-oriented stub (Fig. 1*A*) (25). The type 2-oriented stub can be re-cleaved by BACE1 and ADAM17 to release a soluble EGF-like domain, capable of paracrine signaling (24). Both membrane-tethered stubs may undergo further cleavage for degradation/signaling by I-CLiPs. For the type 1-oriented stub, evidence exists that γ-secretase liberates an ICD, which is required for reverse signaling (26, 27). Furthermore, a schizophrenia-associated single nucleotide polymorphism (SNP; valine to leucine) close to the C-terminal end of the NRG1 type III TMD (Fig. 1*A*) (28) appears to result in an accumulation of the type 1-oriented CTF (29), suggesting that γ-secretase cleavage is disturbed. Consistent with that finding, BACE1 knock-out mice exhibit schizophrenia-like behavioral phenotypes (30).

We now demonstrate that NRG1 type III is the first protein that is a substrate for three different I-CLiPs, namely γ-secretase, SPPL2a, and SPPL2b. Moreover, we identified the corresponding cleavage sites and could show that the valine to leucine exchange, which is associated with schizophrenia, is only one amino acid C-terminal to the initial cleavage site of γ-secretase. Furthermore, this mutation not only reduces generation of the NRG1 type III β-peptide (NRG1-β) and signaling via the ICD but also affects the cleavage precision of γ-secretase.

Experimental Procedures

cDNA Constructs, Primers, Lentivirus Production, and Recombinant NRG1 β-Peptide—Generation of the rat NRG1 type III β1a (GenBank™ accession number AF194438.1) cDNA construct and the V5-NRG1 type III cDNA construct containing an N-terminal V5 tag (GKPIPNPLLGLDST) has been described before (24). The FNRGΔC-HA construct was generated via PCR by inserting into the pSecTag2A vector (Life Technologies, Inc.) the sequence of the NRG1 type III C-terminal transmembrane domain from the BACE1 cleavage site in the stalk region (Met-294) to Lys-334 in the intracellular domain. A FLAG tag (DYKDDDDK) and a linker (IM) were inserted immediately N-terminal of Met-294. At the C terminus (Lys-334) a linker (GG) and an HA tag (YPYDVPDYA) followed by two proline residues (to prevent degradation) were added. The FNRGΔE construct contains the entire C-terminal sequence of NRG1 type III β1a starting with Met-294. This sequence was inserted into the pSecTag2A vector by PCR, and a FLAG tag with a linker (IM) was inserted N-terminal to Met-294. The FNRG-NTF-V5 construct bears an N-terminal FLAG tag after Met-1 and otherwise represents a C-terminally truncated version of NRG1 type III β1a comprising the first 114 residues followed by a V5 tag. The construct was generated by PCR and cloned into the pcDNA3.1hygro+ vector (Life Technologies, Inc.). For matrix-assisted laser desorption/ionization-time of flight (MALDI-TOF) mass spectrometry (MS) analysis of the NRG1 C-peptides, the V5-NRG-NTF-FLAG construct was generated by inverting the tags of FNRG-NTF-V5 and adding an alanine-proline motif at the C terminus to prevent degradation by carboxypeptidases in cell culture supernatants (19). The BACE1 cDNA construct was described previously (31) as were the lentiviral expression construct NRG1 type III and the production of lentiviral particles (24). The schizophrenia-associated Val to Leu mutation was introduced into the respective constructs by QuikChange mutagenesis (Stratagene). All cDNA constructs were verified by sequencing (oligonucleotide sequences are available upon request). The synthetic NRG1 β-peptide used as control includes residues Met-294–Val-316 of NRG1 type III (MEAEELYQKRVLTITGICIALLV) and was obtained from IRIS Biotech GmbH.

Stable Cell Lines, Transfection, and Inhibitor Treatment—HEK293 cells were cultured in DMEM with GlutaMAX (Life Technologies, Inc.) supplemented with 10% fetal calf serum (Sigma). HEK293 cells stably expressing wild-type PS1 or the inactive mutant PS1 D385N were described before (32, 33). Likewise, HEK293 cells inducibly overexpressing untagged human SPP as well as C-terminally HA-tagged human SPPL2a, SPPL2b, and SPPL3 and the respective active site mutants were described previously (34–36). To induce protease expression, the culture medium was supplemented with 1 μg/ml doxycycline (BD Biosciences) for at least 48 h before analysis. All transient transfections were performed using Lipofectamine 2000 (Life Technologies, Inc.) following the manufacturer's instructions. For protease inhibitor experiments, fresh medium with or without inhibitor was added for 16–24 h. The following inhibitors were dissolved in DMSO and used at the indicated final concentrations: γ-secretase inhibitor DAPT

(5 μM, Boehringer-Ingelheim), BACE1 inhibitor IV (5 μM, Calbiochem), SPP and SPPL2a/2b inhibitor $(Z\text{-}LL)_2$ ketone (20 μM, Calbiochem).

Primary Neuronal Culture, Transduction, and Inhibitor Treatment—Rat cortical neurons were prepared according to a protocol described previously (37) and were cultured in neurobasal medium supplemented with 2% B27 (Life Technologies, Inc.), penicillin/streptomycin, and 2 mM L-glutamine. At day 4 *in vitro,* lentiviral particles were added to the cells and incubated for 8 h after which the medium was exchanged. After a 2-day recovery period, inhibitor treatment was performed for 16–24 h, and conditioned media and cell lysates were analyzed by immunoblotting as described below.

Antibodies—The monoclonal antibodies (mAbs) 10E8 and 4F10 directed against the BACE1-cleaved neoepitopes in the NRG1 type III stalk region were described earlier (24) as was the mAb specific for human SPPL3 (clone 7F9) (35). The SPP antibody (clone SPP2:5H7) was generated in rat and is directed against the linear epitope RFDISLKKNTHTYF (amino acids 278–291) of human SPP. The following commercial antibodies were used: α-V5 tag (mouse mAb, 2F11F7, Life Technologies, Inc.; 1:5000); α-FLAG tag (rabbit pAb, F-7425, and mouse mAb, M2, Sigma; 1:5000); α-HA tag (rat mAb, 3F10, Roche Applied Science, and rabbit pAb, 6908, Sigma; 1:5000); α-NRG1 C terminus (rabbit pAb, SC348, Santa Cruz Biotechnology; 1:2000–10,000); α-calnexin (rabbit pAb, Enzo Life Sciences; 1:5000); α-actin (mouse, mAb, Sigma; 1:5000); and α-APP C terminus (rabbit pAb, Sigma; 1:1000). Secondary antibodies were HRP-conjugated to α-mouse and α-rabbit IgG (goat pAb, Promega; 1:10,000) or α-rat IgG (goat pAb, sc-2006, Santa Cruz Biotechnology; 1:4000).

Cell-free γ-Secretase Assay—The cell-free γ-secretase assay used to generate the NRG1 ICD *in vitro* was modified from a protocol published previously (38). Briefly, post-nuclear supernatants were prepared from HEK293 cell lysates by centrifugation (10 min, 1000 × *g*, 4 °C), and cell membranes were isolated by ultracentrifugation (1 h, 100,000 × *g*, 4 °C). Membranes were resuspended in 100 μl of assay buffer (150 mM sodium citrate, pH 6.4, 5 mM 1,10-phenanthroline, supplemented with 4× protease inhibitor (Roche Applied Science)) and incubated with agitation at 37 or 4 °C for 3.5 h. The γ-secretase inhibitor L-685,458 (Calbiochem) was added to a final concentration of 1 μM. The reaction was terminated by placing the samples on ice, and membranes (P100) and supernatants (S100) were separated by ultracentrifugation (1 h, 100,000 × *g*, 4 °C). Membrane pellets were solubilized in lysis buffer (20 mM sodium citrate, pH 6.4, 1 mM EDTA, 1% Triton X-100, protease inhibitor (Sigma)) and analyzed by SDS-PAGE and immunoblotting. The S100 fraction containing the NRG1 ICD was either subjected to immunoblot analysis or further processed and analyzed by mass spectrometry.

Sample Preparation, Immunoprecipitation, and Immunoblotting—Preparation of cell lysates and conditioned media as well as sample analysis by SDS-PAGE and immunoblotting were performed as described (24) unless otherwise specified. For immunoprecipitation, conditioned media were pre-cleared with 2–5 μl/ml (at least 20 μl) protein G-Sepharose (protein G-Sepharose 4 Fast Flow, GE Healthcare) for 1 h (all steps at 4 °C with overhead rotation). Thereafter, antibody was added to the pre-cleared conditioned media, and the sample was incubated overnight. After antibody binding protein G-Sepharose was added, incubated for at least 3 h, and collected by centrifugation (5 min at 2000 × *g*). The following antibodies were used as agarose bead conjugates, similarly incubated overnight, and also collected by centrifugation: α-FLAG tag (mouse mAb, M2, Sigma) and α-HA tag (mouse mAb, HA-7, Sigma). Beads were washed two times with STEN buffer (50 mM Tris, pH 7.6, 150 mM NaCl, 2 mM EDTA, 0.2% Nonidet P-40) and H_2O and eluted with SDS-PAGE sample loading buffer for 5 min at 95 °C, and isolated proteins were analyzed by immunoblotting. NRG1-β was separated on Tris-Tricine gels (10–20%, Life Technologies, Inc.) and transferred to nitrocellulose membranes (0.1 μm, GE Healthcare). Upon completion of the transfer and prior to incubation with blocking solution, NRG1-β was additionally denatured by boiling the nitrocellulose membrane in PBS for 5 min. To detect the N-terminal NRG1, ICDs generated by SPPL2a/2b-mediated intramembrane cleavage of V5-NRG1 type III cell membranes were isolated as described (36).

Immunoprecipitation (IP) and Mass Spectrometric Analysis—IP coupled to MS analysis was performed as described previously (24, 39) using an α-cyano-4-hydroxycinnamic acid matrix (in 0.3% trifluoroacetic acid, 40% acetonitrile, H_2O) and a MALDI-TOF Voyager DE STR mass spectrometer (Applied Biosystems). Molecular masses were calibrated with the Sequazyme™ peptide mass standards kit (Applied Biosystems). For mass spectrometric analysis of the NRG1-β, conditioned media were immunoprecipitated with the 10E8 antibody and 20 μl of protein G-Sepharose as described above. The NRG1 C-peptide peptide and the ΔNRG1-β peptide were precipitated with 20 μl of α-FLAG tag agarose beads (mouse mAb, M2, Sigma). After collection, beads were washed three times with IP-MS buffer (10 mM Tris, pH 8.0, 140 mM NaCl, 5 mM EDTA, 0.1% octyl β-D-glucopyranoside) and two times with H_2O. Bound NRG1-β and C-peptides were reduced and eluted by adding 30 μl of 75 mM DTT to the agarose beads and incubating the sample for 1 h at 30 °C (with agitation). After centrifugation (1 min, 17,000 × *g* at room temperature), the DTT solution was aspirated, transferred to new reaction tubes, and evaporated using a centrifugal evaporator (20 min, 45 °C). The dried protein was solubilized in 15 μl of the matrix solution. To detect peptides still bound to the agarose beads, the latter were eluted for 5 min at room temperature in 15–20 μl of the matrix. Both samples were transferred to a target plate and analyzed by MALDI-TOF MS. NRG1 ICDs generated with the cell-free γ-secretase assay were reduced and alkylated prior to analysis by MS. Briefly, the S100 assay fraction was adjusted to a final concentration of 50 mM NH_4CO_3 (final pH 7.5–8.5); DTT was added (5.5 mM final concentration), and the sample was incubated for 45 min at 37 °C (all steps with agitation). Alkylation was performed with 10 mM IAA for 45 min at 37 °C in the dark, and excess IAA was subsequently quenched with 16 mM cysteine for 5 min at room temperature. Afterward, 1 ml of IP-MS buffer was added to the sample, and ICDs were immunoprecipitated with α-HA-agarose (mouse mAb, HA-7, Sigma). The beads were washed with IP-MS buffer and eluted with matrix solution as described above.

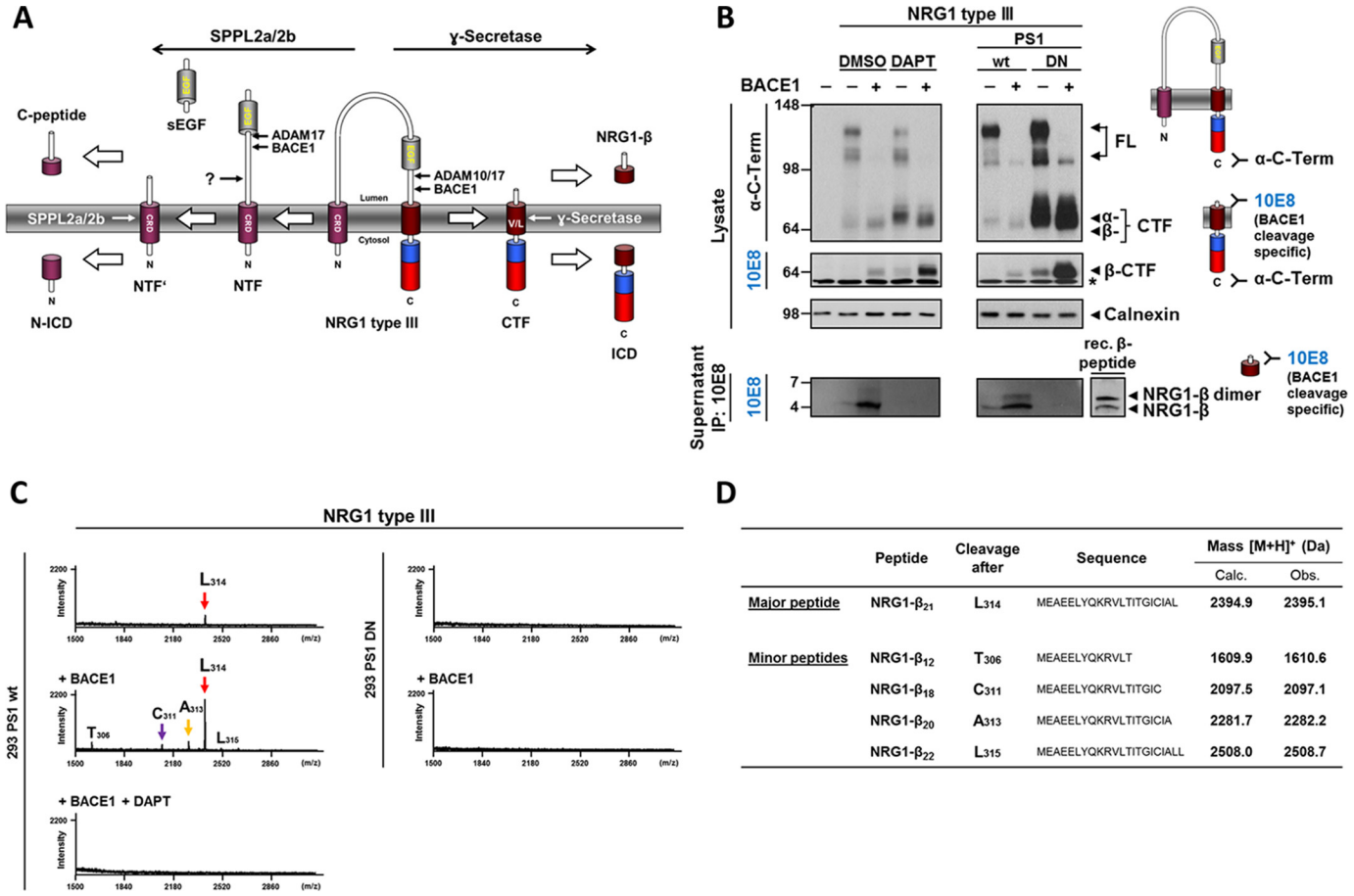

	Peptide	Cleavage after	Sequence	Mass [M+H]⁺ (Da) Calc.	Obs.
Major peptide	NRG1-β_{21}	L_{314}	MEAEELYQKRVLTITGICIAL	2394.9	2395.1
Minor peptides	NRG1-β_{12}	T_{306}	MEAEELYQKRVLT	1609.9	1610.6
	NRG1-β_{18}	C_{311}	MEAEELYQKRVLTITGIC	2097.5	2097.1
	NRG1-β_{20}	A_{313}	MEAEELYQKRVLTITGICIA	2281.7	2282.2
	NRG1-β_{22}	L_{315}	MEAEELYQKRVLTITGICIALL	2508.0	2508.7

FIGURE 1. **γ-Secretase-dependent generation of NRG1-β.** *A,* regulated intramembrane proteolysis of NRG1 type III by three I-CLiPs and at least three sheddases. NTF′ is a novel truncated NTF further described in Fig. 7. *CRD*, cysteine-rich domain; *V/L*, schizophrenia-associated V322L mutation. *B,* γ-Secretase generates soluble NRG1-β from NRG1 CTFs. Wild-type HEK293 cells (*left panel*) and HEK293 cells stably expressing either wild-type (*PS1 wt*) or the proteolytically inactive PS1 D385N mutant (*PS1 DN*) (*right panel*) were transfected with NRG1 type III and with or without BACE1. γ-Secretase activity in wild-type cells (*left panel*) was inhibited with the specific inhibitor DAPT (5 μM). Treatment with DMSO was used as control. Full-length (*FL*) NRG1 type III as well as the C-terminal fragments generated by ADAM10/17 or BACE1 (α-CTF and β-CTF) were detected in the cell lysate with a C-terminal antibody, although the neo-epitope-specific antibody 10E8 selectively detected BACE1-generated β-CTFs. Calnexin was used as a loading control. Secreted NRG1-β was immunoprecipitated and detected using the 10E8 antibody. Enhanced BACE1 expression strongly increased NRG1-β secretion, although inhibition of the γ-secretase (DAPT) or expression of the inactive mutant (*PS1 DN*) abolished its generation. *Asterisk* denotes an unspecific band. *C,* identification of γ-cleavage sites by MALDI-TOF MS. Supernatants of cells transfected with NRG1 type III and with or without BACE1 were immunoprecipitated with antibody 10E8, and isolated peptides were analyzed using MALDI-TOF mass spectrometry. Upon expression of BACE1, the peak intensity of the main cleavage product (*red arrow*) was strongly enhanced, and additional but minor peptides were detected. Inhibition of γ-secretase with DAPT (5 μM) prevented NRG1-β generation as did expression of the catalytically inactive PS1 mutant (*PS1 DN*). *D,* list of identified peptides and comparison of observed peptide masses to the calculated mass. $[M + H]^+$ indicates a singly charged peptide.

NRG1 Cleavage and Nuclear Translocation Assay—The Gal4-VP16 (GV) transcriptional activator was fused to the C terminus of full-length mouse NRG1 type III WT or NRG1 type III Val/Leu (40, 41). PC12 cells were transfected with NRG1-III-GV and reporter constructs containing five clustered Gal4-dependent upstream-activating sequences driving firefly luciferase expression upon GV activity, thus measuring nuclear translocation of ICD-GV (Fig. 5*D*). Bioluminescence was monitored continuously in living cells, using the LumiCycle 32-channel luminometer (Actimetrics), as described previously (42).

Results

γ-Secretase Cleavage Generates a Secreted NRG1 Type III β-Peptide—Ectodomain shedding of NRG1 type III by BACE1 and ADAM proteases generates a membrane-retained β- or α-C-terminal fragment of type 1 orientation (Fig. 1*A*), which is a substrate for intramembrane proteolysis by γ-secretase (26, 27). In analogy to the processing of APP by BACE1 and γ-secretase, which leads to the release of Aβ, we therefore expected the secretion of an Aβ-like peptide of NRG1 type III (NRG1 β-peptide; NRG1-β) (Fig. 1*A*) upon intramembrane processing. To investigate this possibility, we transiently expressed NRG1 type III in HEK293 cells and analyzed cell lysates and conditioned media by Western blotting. Using an antibody against its C terminus, we detected full-length NRG1 type III as two high molecular weight bands, and the NRG1 type III C-terminal fragments at ~64 kDa in the cell lysate (Fig. 1*B*, *left panel*). Co-expression of BACE1 reduced full-length NRG1 type III and led to an enhanced production of the CTF, indicating increased turnover of NRG1 type III by BACE1-mediated shedding (Fig. 1*B*). In line with its role as γ-secretase substrate, treatment of cells with the γ-secretase inhibitor DAPT caused accumulation of the CTF in the cell lysate (Fig. 1*B*). Shedding of NRG1 type III by BACE1 at the β-site and by ADAMs at the α-site results in the generation of β- and α-CTF, respectively

(24, 43). The heterogeneity of these fragments is reflected by their differential migration behavior in Fig. 1*B*. Because BACE1 cleaves closer to the membrane, it creates a smaller β-CTF than ADAM10/17 (α-CTF) (24). To specifically detect the β-CTF, we used the monoclonal antibody 10E8, which selectively recognizes the BACE1-generated N terminus of the β-CTF but does not detect the α-CTF (24). This confirmed increased cleavage of NRG1 type III at the β-site upon co-expression of BACE1 (Fig. 1*B*).

γ-Secretase cleavage is expected to liberate the N terminus of the NRG1 type III β-CTF (Fig. 1*A*). We therefore used antibody 10E8 to immunoprecipitate NRG1-β from conditioned media and indeed detected the peptide as a fragment of ~4 kDa (Fig. 1*B*, *lower panel*). Co-expression of BACE1 strongly increased the amounts of NRG1-β (Fig. 1*B*). Conversely, treatment with the γ-secretase inhibitor DAPT prevented generation of the NRG1-β and caused accumulation of the β-CTF in the cell lysate demonstrating that the identified peptide was generated in a γ-secretase-dependent manner (Fig. 1*B*). This was further confirmed with cells expressing a catalytically inactive PS1 D385N mutant (PS1DN) (44), which prevented the release of NRG1-β and caused the accumulation of CTFs in the cell lysate (Fig. 1*B*, *right panel*). NRG1-β co-migrated with a synthetic peptide containing the 23 residues (Met-294–Val-316) of the stalk immediately C-terminal of the BACE1-shedding site (Phe-293) (24, 45) and the first half of the TMD. This indicates that the γ-cleavage site in NRG1 type III is located close to the middle of the transmembrane domain. Both the synthetic and the secreted peptide migrated as a doublet suggesting dimer formation (Fig. 1*B*). These findings demonstrate that the combined cleavage by BACE1 and γ-secretase releases NRG1-β from NRG1 type III.

Identification of Intramembrane Cleavage Sites in the TMD of the NRG1 Type III CTF—γ-Secretase processes its substrates in a stepwise manner from the ε- to the γ-site in the C-terminal half of the TMD and then releases small peptides like Aβ into the luminal space (8–10). To identify the γ-cleavage site within the TMD of the NRG1 type III CTF, we immunoprecipitated NRG1-β from conditioned media with antibody 10E8 and performed mass spectrometric analysis. One peptide with a molecular mass of 2395.1 Da was identified in the conditioned media of HEK293 cells expressing NRG1 type III (Fig. 1, *C* and *D*). Its molecular mass corresponds to a peptide comprising residues Met-294 to Leu-314 indicating γ-secretase cleavage 21 residues C-terminal of the BACE1 cleavage site after Leu-314 (Fig. 1*D*, see also Figs. 3 and 4). Enhanced shedding upon overexpression of BACE1 strongly increased generation of this peptide and revealed additional minor cleavage products (Fig. 1, *C* and *D*). Mass spectrometric analysis of conditioned media from cells treated with DAPT or expressing a catalytically inactive γ-secretase variant (PS1DN) revealed no signals, confirming again the γ-secretase dependence of the NRG1 β-peptide secretion (Fig. 1*C*). In summary, we identified Leu-314 as a major γ-secretase cleavage site responsible for the release of NRG1-β and showed that this peptide includes 21 residues (Met-294–Leu-314). Leu-314 is located almost equidistantly from the luminal and cytoplasmic border of the NRG1 type III C-terminal TMD at a position similar to the γ-secretase cleavage site in APP that leads to the generation of Aβ (compare with Figs. 4*C* and 10).

Primary Neurons Process NRG1 Type III to Release NRG1-β—To confirm that endogenous proteases in neurons also process NRG1 type III to release NRG1-β, we expressed NRG1 type III in primary cortical neurons via lentiviral delivery. Both full-length NRG1 type III and CTFs (α- and β-CTF) were readily detected in the cell lysates by an antibody to the C terminus of NRG1 type III (Fig. 2*A*). The neo-epitope-specific antibody 10E8 was used to specifically detect the BACE1-generated β-CTFs. Treatment with a BACE1 inhibitor (BACE1 inhibitor IV) abolished shedding by BACE1 as evidenced by the absence of the BACE1-generated β-CTF and the accumulation of the full-length protein. The slightly larger α-CTFs that remain after BACE1 inhibition are generated through shedding by compensating ADAM secretases at the α-site of NRG1 type III (24, 43). As expected, blocking γ-secretase with DAPT resulted in elevated levels of CTFs but had no effect on full-length NRG1 type III. Immunoprecipitation and Western blotting with the 10E8 antibody revealed NRG1-β in the supernatant of neurons expressing NRG1 type III (Fig. 2*A*, *lower panel*). NRG1-β was absent in the medium of neurons treated with BACE1 or γ-secretase inhibitors (Fig. 2*A*, *lower panel*). Together, these results demonstrate that NRG1 type III is processed in neurons by endogenous BACE1 and γ-secretase to release soluble NRG1-β.

To demonstrate that not only overexpressed but also endogenous NRG1 type III is processed by γ-secretase, we treated neurons with DAPT. Under these conditions the endogenous NRG1-derived CTFs but not NTFs accumulated (Fig. 2*B*) demonstrating that NRG1 type III is a physiological substrate of γ-secretase. Accumulation of APP CTFs upon DAPT treatment served as a control (Fig. 2*B*).

γ-Secretase Cleaves the NRG1 Type III CTF at an ε-Site to Release the NRG1 ICD—After identifying the γ-cleavage sites (Fig. 1, *C* and *D*), we went on and determined the cleavage site(s), which allows liberation of the NRG1 ICD. We used a well characterized cell-free γ-secretase assay (38) to generate the NRG1 ICD for mass spectrometric analysis. To this end we constructed FNRGΔC-HA, which includes an N-terminal FLAG tag followed by a short extracellular part, the TMD, a short intracellular part, as well as a C-terminal HA tag (Fig. 3*A*). Truncation of the intracellular domain of NRG1 type III was necessary because the authentic domain (~64 kDa) is too large to allow an exact molecular mass determination by MALDI-TOF MS. Because of the short extracellular domain, γ-secretase cleavage of FNRGΔC-HA does not depend on shedding. Western blot analysis of the soluble fraction of the *in vitro* assay performed with wild-type or non-functional mutant (PS1DN) γ-secretase revealed *de novo* generation of NRG1 ICD(ΔC) in a γ-secretase-dependent manner (Fig. 3*B*). This was further confirmed by blocking γ-secretase cleavage with the specific inhibitor L-685,458, which abolished the generation of NRG1 ICD(ΔC) (Fig. 3*B*). In addition to the NRG1 ICD(ΔC), intramembrane cleavage of FNRGΔC-HA also generates a membrane-retained N-terminal fragment corresponding to a truncated NRG1-β (ΔNRG1-β). Probably due to its hydrophobicity, this fragment was detected in the insoluble fraction.

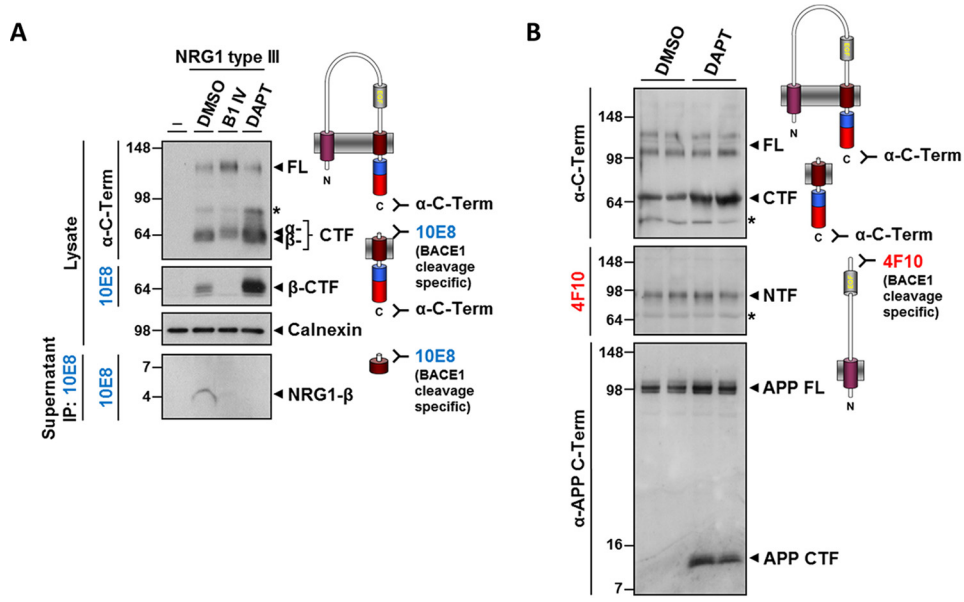

FIGURE 2. **γ-Secretase-mediated processing of NRG1 type III in primary neurons.** *A,* proteolytic generation of NRG1-β in primary cortical neurons. NRG1 type III was expressed in primary rat cortical neurons using lentiviral transduction. Cells were treated with a BACE1 inhibitor (*B1 IV*, 5 μM), a γ-secretase inhibitor (DAPT, 5 μM), or DMSO as control. Full-length (*FL*) protein and the CTFs of NRG1 type III were detected in the cell lysate using an antibody against the C terminus. The neo-epitope antibody 10E8 was used to specifically visualize the BACE1-generated β-CTFs. Calnexin served as loading control. After immunoprecipitation with the 10E8 antibody NRG1-β was detected in the supernatant of control cells. Inhibition of BACE1 abolished generation of the β-CTF and consequently secretion of NRG1-β. Treatment with DAPT caused accumulation of CTFs and prevented their turnover to NRG1-β by γ-secretase. *Asterisk* denotes a longer CTF probably generated by the BACE1/ADAM17 cleavage N-terminal to the EGF-like domain. *B,* proteolytic turnover of the NRG1 CTF by γ-secretase. Neurons were treated with DAPT (5 μM) or DMSO as control, and proteins were detected in the cell lysate as before. Note that the NRG1 CTF but not the NRG1 NTF accumulates upon inhibition of γ-secretase. Accumulation of APP CTFs upon DAPT treatment served as a control. *Asterisk* denotes an unspecific band.

Generation of ΔNRG1-β depended on an active γ-secretase as its production is prevented in *in vitro* assays using membranes derived from cells expressing catalytically inactive PS1DN (Fig. 3*B*).

To determine the position of the ϵ-like cleavage site, the NRG1 ICD(ΔC) was immunoprecipitated from the soluble fraction using α-HA-agarose beads, and the isolated peptides were analyzed by MALDI-TOF MS (Fig. 3*C*). A major peak was observed at a molecular mass of 3030.4 Da corresponding to cleavage of the peptide bond between Cys-321 and Val-322 (Fig. 3, *C* and *D*). No peptides were detected when the *in vitro* assay was carried out in the presence of the γ-secretase inhibitor L-685,458, at 4 °C, or when the PS1 loss-of-function mutation PS1DN was expressed (Fig. 3*C*) demonstrating that cleavage at the identified ϵ-like site is mediated by γ-secretase.

Because different substrates were used to determine the ϵ- and γ-cleavage sites (truncated FNRGΔC-HA *versus* full-length NRG1 type III), we confirmed the position of the γ-cleavage in the truncated FNRGΔC-HA by MALDI-TOF MS. This revealed that the cleavage sites were very similar, although the ratio of the individual cleavages shifted slightly so that cleavage after leucine 315 became more prominent (Fig. 4, *A* and *B*). Such minor changes in the quantitative but not qualitative cleavage pattern are probably due to slight differences in substrate positioning at the active site of γ-secretase or antibodies used for immunoprecipitation and have been described before for a truncated Notch1 substrate (39, 46).

Taken together, these results suggest that the NRG1 type III ICD is released into the cytosol through intramembrane cleavage at an ϵ-like site located in close proximity to the cytosolic membrane border, whereas the γ-cleavage, which releases NRG1-β, occurs within the middle of the TMD (Fig. 4*C*).

Single Nucleotide Polymorphism Associated with Schizophrenia Is Located at the ϵ-Like Site and Impairs γ- and ϵ-Cleavage—NRG1 is a major susceptibility gene for schizophrenia, and many disease-associated SNPs have been identified (47, 48). Whereas most disease-associated SNPs are located in non-coding regions of the *NRG1* gene, one SNP causes a valine to leucine exchange at amino acid 322 in the C-terminal TMD of NRG1 (28). Interestingly, this mutation is located immediately C-terminal of the ϵ-like cleavage site identified in Fig. 3 and could therefore impact proteolysis by γ-secretase. Indeed, previous experiments in cell culture have shown that the valine to leucine mutation causes an accumulation of the NRG1 CTF while leaving the levels of the full-length precursor unaffected (29). Because this is indicative of an impaired turnover of the mutant NRG1 CTF, we wanted to investigate its impact on γ-secretase cleavage in more detail. To this end we generated an NRG1 type III construct harboring the valine to leucine mutation (NRG1 type III VL) and expressed it in HEK293 cells. Compared with cells expressing wild-type NRG1 type III, we detected slightly increased levels of CTFs in cells expressing the mutant protein (Fig. 5*A*). Co-expression of BACE1 led to a complete turnover of the full-length precursor and exacerbated the difference in the levels of wild-type and mutant CTFs. This suggests that the valine to leucine mutation leads to a reduction of γ-secretase cleavage and therefore to an accumulation of the CTFs. When cleavage by the γ-secretase was blocked pharmacologically using the inhibitor DAPT, equal levels of CTFs were detected in cells expressing the

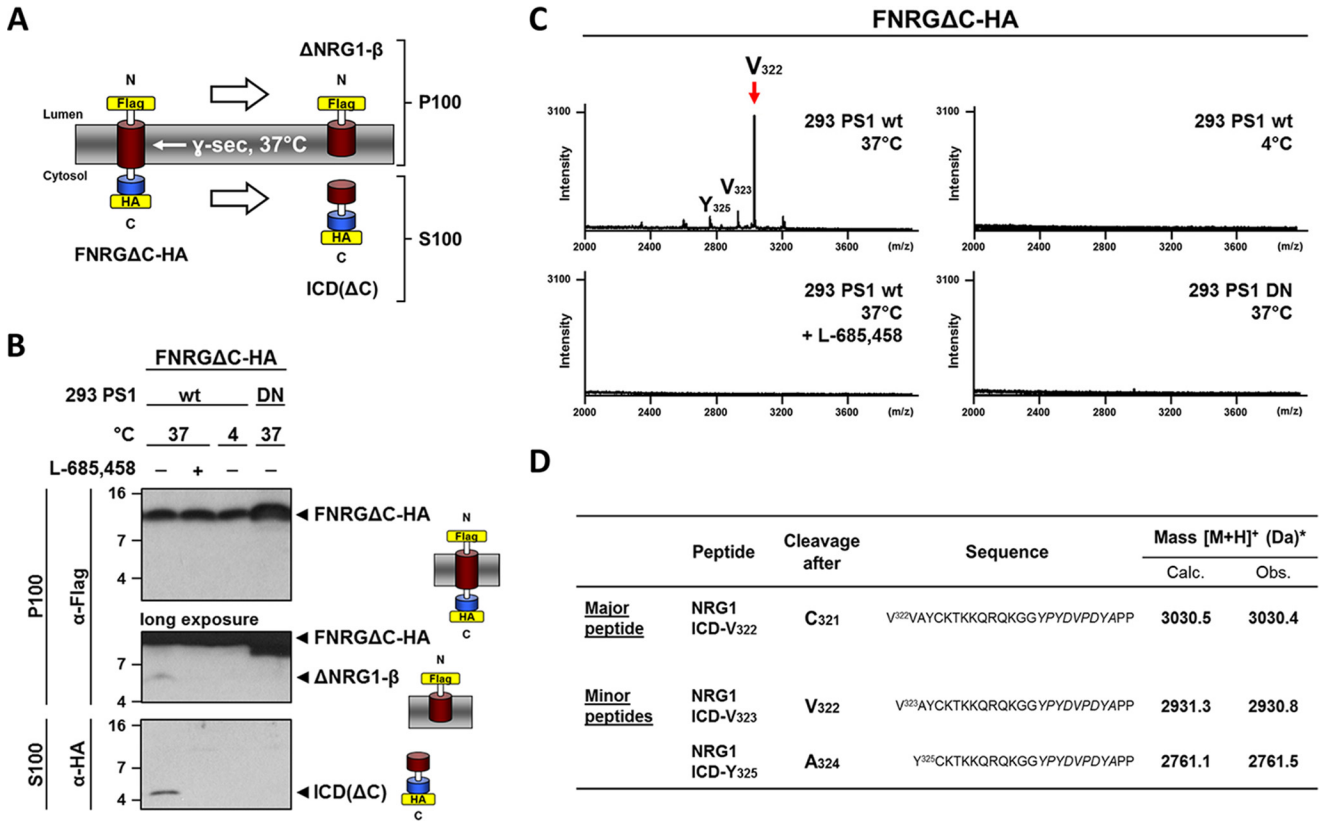

	Peptide	Cleavage after	Sequence	Mass [M+H]⁺ (Da)*	
				Calc.	Obs.
Major peptide	NRG1 ICD-V322	C321	V322VAYCKTKKQRQKGG*YPYDVPDYA*PP	3030.5	3030.4
Minor peptides	NRG1 ICD-V323	V322	V323AYCKTKKQRQKGG*YPYDVPDYA*PP	2931.3	2930.8
	NRG1 ICD-Y325	A324	Y325CKTKKQRQKGG*YPYDVPDYA*PP	2761.1	2761.5

FIGURE 3. **Generation of the NRG1 type III ICD by γ-secretase and identification of the ϵ-cleavage site.** *A,* schematic overview of the cell-free γ-secretase *in vitro* assay. *B,* generation of the NRG1 ICD by γ-secretase in a cell-free assay. FNRGΔC-HA was expressed in cells stably expressing either wild-type or a catalytically inactive (*DN*) PS1 mutant. Cell membranes were used for the *in vitro* assay at indicated temperatures. L-685,458 (1 μM) blocked γ-secretase activity in the *in vitro* assay containing membranes derived from cells expressing wild-type PS1. *C,* identification of the ϵ-cleavage site in the C-terminal TMD of NRG1 type III by MALDI-TOF mass spectrometry. The soluble fraction (*S100*) shown in *B* was immunoprecipitated with α-HA-agarose, and isolated peptides were analyzed using MALDI-TOF mass spectrometry. A peptide generated by cleavage after Cys-321 (*red arrow*) was only detected when the assay was performed with wild-type γ-secretase at 37 °C. Addition of the γ-secretase inhibitor L-685,458 or expression of the catalytically inactive γ-secretase (*PS1DN*) abolished all signals. *D,* list of identified peptides and comparison of observed peptide mass with the calculated mass. Note that two proline residues at the C terminus of FNRGΔC-HA were added to prevent degradation. *Asterisk,* because of alkylation with IAA prior to MS analysis, the mass of each peptide is increased by 58.0 Da per cysteine residue. *Italic letters* indicate the HA tag, $[M + H]^+$, a singly charged peptide.

wild-type and mutant NRG1 type III protein (Fig. 5*A*). Together, this demonstrates that the valine to leucine mutation causes accumulation of the CTF by impairing γ-secretase cleavage but not by increasing shedding of full-length NRG1 type III (this is further confirmed by expressing FNRGΔE, see Fig. 5*B*).

As we discovered that γ-secretase cleavage of the NRG1 type III CTF releases NRG1-β (Figs. 1*B* and 2*A*), we asked whether the valine to leucine mutation also affects NRG1-β generation. To allow a quantitative detection of the NRG1 β-peptide, we generated the FNRGΔE construct, which includes the entire CTF but lacks the ectodomain of NRG1 type III (Fig. 5*B*). Because of its extracellular truncation, FNRGΔE is a direct substrate for the γ-secretase and enables investigation of the valine to leucine mutation independent of shedding. Transfection of HEK293 cells with FNRGΔE allowed robust expression, and the construct's N-terminal FLAG tag allowed detection of secreted NRG1-β in the cell culture media without prior immunoprecipitation. Supernatants from cells expressing the valine to leucine mutant of FNRGΔE contained significantly less NRG1-β compared with cells expressing the wild-type construct while simultaneously increased amounts of the uncleaved precursor protein were detected (Fig. 5, *B* and *C*). The FLAG-tagged peptide was detected as a monomer and higher, probably oligomeric, molecular weight forms (Fig. 5*B*). As expected, generation of NRG1-β was blocked upon treatment of cells with the γ-secretase inhibitor DAPT (Fig. 5*B*). Together, these results demonstrate that the schizophrenia-associated valine to leucine mutation close to the ϵ-like site in the TMD of NRG1 type III impairs processing and release of NRG1-β by γ-secretase. These findings are consistent with the previously observed increase of mutant NRG1 CTFs (29).

Furthermore, the valine to leucine mutation not only reduces NRG1-β generation by cleavage at the γ-site but also affects ϵ-cleavage. This was shown by a live-cell reporter assay allowing us to measure NRG1 cleavage and nuclear translocation of the released NRG1 ICD. As shown in Fig. 5, *D* and *E*, γ-secretase-dependent processing of the NRG1 valine to leucine mutation at the ϵ-cleavage site is reduced by ~30% and by more than 50% upon BACE1 co-expression. Treatment with the γ-secretase inhibitor DAPT abrogated the observed ICD signaling confirming the γ-secretase dependence of the NRG1 ICD generation. Thus, the mutation reduces both the initial ϵ-cleavage giving rise to the ICD as well as the final γ-cleavage resulting in the release of NRG1-β.

A

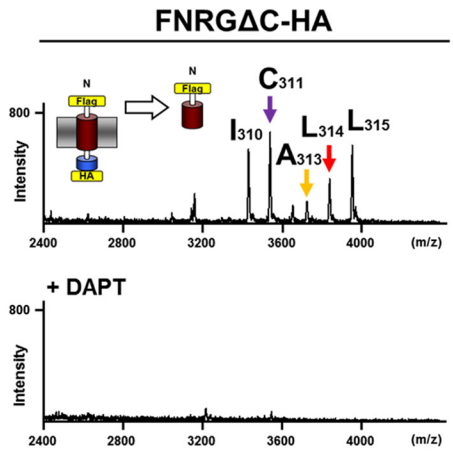

B

Peptide	Cleavage after	Sequence	Mass [M+H]+ (Da)	
			Calc.	Obs.
NRG1-β_{22}	L_{315}	SL*DYKDDDD*KIMMEAEELYQKRVLTITGICIALL	3947.6	3951.1
NRG1-β_{21}	L_{314}	SL*DYKDDDD*KIMMEAEELYQKRVLTITGICIAL	3834.4	3837.2
NRG1-β_{20}	A_{313}	SL*DYKDDDD*KIMMEAEELYQKRVLTITGICIA	3721.3	3723.4
NRG1-β_{18}	C_{311}	SL*DYKDDDD*KIMMEAEELYQKRVLTITGIC	3537.1	3539.3
NRG1-β_{17}	I_{310}	SL*DYKDDDD*KIMMEAEELYQKRVLTITGI	3433.9	3433.5

C

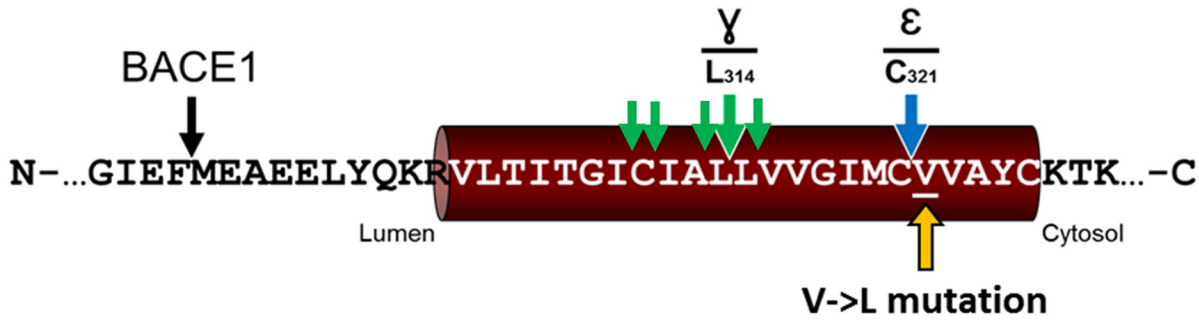

FIGURE 4. **γ-Secretase processes FNRGΔC-HA at the γ-cleavage site similar to NRG1 type III.** *A,* identification of the γ-cleavage sites of FNRGΔC-HA by mass spectrometry. γ-Secretase cleavage in cells expressing FNRGΔC-HA releases FLAG-tagged ΔNRG1-β peptides into the cell culture media. ΔNRG1-β peptides were immunoprecipitated with α-FLAG-agarose, and isolated peptides were analyzed using MALDI-TOF mass spectrometry. Treatment with the γ-secretase inhibitor DAPT (5 μM) prevented ΔNRG1-β generation. *B,* list of identified peptides and comparison of observed peptide mass to the calculated mass. *Italic letters* indicate the FLAG tag, which is followed by a linker (IM); $[M + H]^+$ indicates a singly charged peptide. *C,* schematic presentation of the γ-secretase cleavage sites within the C-terminal TMD (*brown*) of NRG1 type III as determined in Figs. 1 and 3. γ- and ε-cleavage sites are indicated by *green* and *blue arrows*, respectively. The BACE1 cleavage site is shown for reference. A mutation caused by an SNP genetically linked to an increased risk of schizophrenia is located only one amino acid C-terminal of the ε-cleavage site (*yellow arrow*).

Schizophrenia-associated Valine to Leucine Mutation in NRG1 Type III Alters the Cleavage Precision of γ-Secretase—As we observed impaired γ-secretase processing of the mutant NRG1 type III, we investigated whether the valine to leucine mutation affects not only the extent but also the precision of the γ-secretase cleavage similar to the mutations occurring in APP (49). To this end NRG1-β was isolated from the supernatants of HEK293 cells expressing BACE1 and wild-type or mutant NRG1 type III as described above and analyzed by MALDI-TOF mass spectrometry (Fig. 6*A*). Consistent with our findings in Fig. 1, *C* and *D,* one major and several minor NRG1-β species were observed in the supernatants of cells expressing wild-type NRG1 type III (Fig. 6*A*). The most abundant NRG1-β21 peptide is generated by γ-secretase cleavage after Leu-314, whereas the shorter NRG1 β-peptides NRG1-β20 and -β18 are derived from cleavages after Ala-313 and Cys-311, respectively (compare Fig. 1, *C* and *D*). Interestingly, an increase in the amount of the NRG1-β20 relative to the NRG1-β21 peptide was evident in the mass spectra from supernatants of cells expressing the NRG1 type III valine to leucine mutant (Fig. 6*A*). Using a semi-quantitative approach, we determined the abundance of the individual peptides by measuring the areas under the respective peaks and normalizing to the combined signal (total area) derived from all NRG1-β species (Fig. 6*B*). This revealed that the valine to leucine mutation leads to an increase in the abundance of the NRG1-β20 peptide (27% *versus* 13% wild type) and to a concomitant decrease of the NRG1-β21 peptide (68% *versus* 83% wild type). Thus, the valine to leucine mutation in NRG1 type III shifts the cleavage precision of the γ-secretase from Leu-314 to Ala-313 and consequently the ratio of the secreted peptides from NRG1-β21 to NRG1-β20 (Fig. 6*C*).

N-terminal Stub of NRG1 Type III Is an SPPL2a and SPPL2b Substrate—Because type 2-oriented membrane proteins can be processed by members of the SPP/SPPL I-CLiP subfamily (13), we co-expressed N-terminally V5-tagged NRG1 type III (V5-NRG1 type III) with SPP, SPPL2a, SPPL2b, and SPPL3 as well as their corresponding catalytically inactive aspartyl mutations (DA, Fig. 7*A*) (50). Consistent with the results described above, we detected full-length NRG1 type III as two closely spaced high molecular weight bands (Fig. 7*A*). In line with our previous observation (24), we also detect the NRG1 type III NTF at around 80 kDa (Fig. 7*A*). In addition, we identified a novel smaller protein fragment of ~28 kDa (Fig. 7*A*). As this fragment retains V5 immunoreactivity, we reasoned that it must originate from a C-terminal truncation of NRG1 type III and will

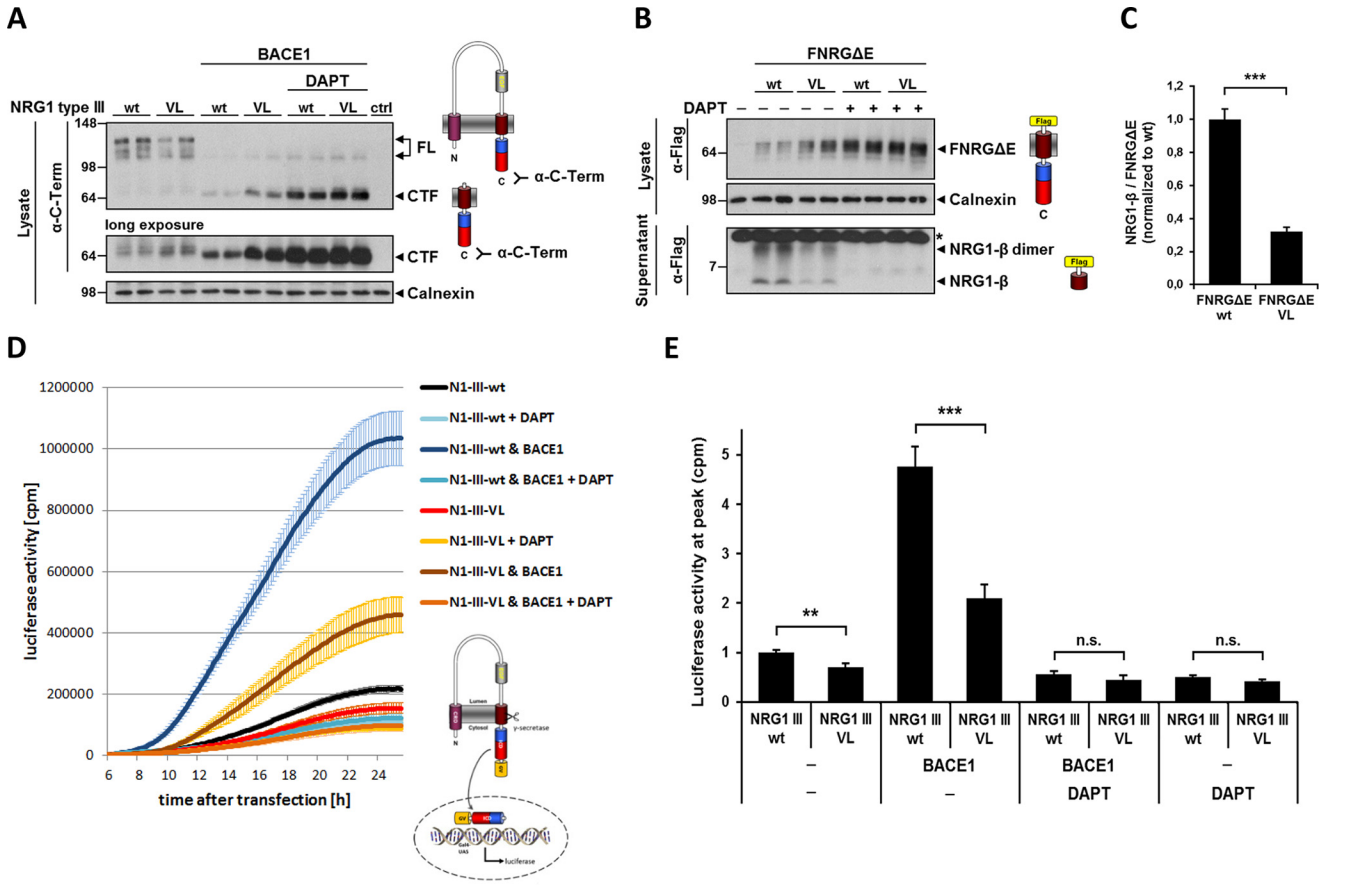

FIGURE 5. **Schizophrenia-associated Val to Leu mutation impairs γ-secretase cleavage and generation of NRG1-β and NRG1 ICD.** *A,* Val to Leu mutation inhibits processing of the NRG1 type III CTF by γ-secretase. Wild-type and mutant (VL) NRG1 type III were expressed in HEK293 cells with or without BACE1. Cell lysates were prepared, and full-length NRG1 type III and CTFs were detected with a C-terminal antibody. CTFs accumulated in cells expressing the mutant as compared with the wild-type NRG1 type III. Inhibition of γ-secretase cleavage (DAPT, 5 μM) led to further increased but equal levels of CTFs in NRG1 type III wild-type and VL mutant cells. Calnexin was used as loading control. *B,* reduced generation of NRG1-β in cells expressing the VL mutant. FNRGΔE was expressed in HEK293 cells and the N-terminal FLAG tag was used for direct detection of NRG1-β in the supernatant. Significantly more NRG1-β was released from cells expressing the wild-type construct compared with the mutant. Simultaneously, the mutant FNRGΔE precursor accumulated in the cell lysate. Inhibition of γ-secretase with DAPT abolished generation of the NRG1-β and led to increased but equal levels of FNRGΔE wild-type and VL. Calnexin was used as loading control. *Asterisk* denotes an unspecific band. *C,* quantification from three independent experiments: mean ± S.D., ***, $p < 0.001$, two-tailed unpaired Student's *t* test. *D* and *E,* generation and nuclear translocation of the NRG1 type III ICD is impaired by the Val to Leu mutation. A live-cell reporter assay shows reduced generation and translocation of the NRG1 ICD from the Val to Leu mutant (NRG1 III VL) compared with the wild-type (*NRG1 III wt*). This effect was particularly pronounced when shedding was enhanced by BACE1 co-expression. Conversely, upon DAPT treatment the signal was equally reduced with or without BACE1 co-expression, demonstrating the γ-secretase dependence of reduced NRG1 III VL processing. Quantification of luciferase activity was done 24 h after transfection. *n.s.,* not significant by Student's *t* test.

refer to this protein fragment as NTF′. Because the molecular weight of NTF′ is too small to be derived from the dual BACE1 cleavage (24), it is likely that an additional shedding event generates the smaller 28-kDa NTF′ fragment from the NTF (see also Fig. 1*A*). Upon co-expression of V5-NRG1 type III with wild-type SPPL2a and SPPL2b, NTF′ was reduced, and a smaller peptide appeared indicating a precursor product relation (Fig. 7*A*). As this fragment was absent in cells that express catalytically inactive SPPL2a (D412A) or SPPL2b (D421A) (Fig. 7*A*), it likely represents an N-terminal ICD (N-ICD) generated by SPPL2a/SPPL2b. Co-expression of V5-NRG1 type III with either SPPL3 or SPP did not allow N-ICD generation (Fig. 7*A*). To further substantiate that the generation of N-ICD is dependent on the catalytic activity of SPPL2a or SPPL2b, the $(Z\text{-}LL)_2$ ketone was used to inhibit the proteolytic activity of the ectopically expressed I-CLiPs. The $(Z\text{-}LL)_2$ ketone was initially identified as an inhibitor of SPP activity (14) but also potently inhibits its proteolytic processing of TNFα (16) and Bri2 (34) by SPPL2a or SPPL2b. Although the NTF′ of NRG1 type III was turned over in cells co-expressing active SPPL2a or SPPL2b, treatment of these cells with $(Z\text{-}LL)_2$ ketone strongly reduced N-ICD levels and resulted in the accumulation of the NTF′ (Fig. 7*B*). This demonstrates that the catalytic activity of SPPL2a or SPPL2b is essential for N-ICD production. Taken together, these findings demonstrate that NRG1 type III is cleaved by SPPL2a or SPPL2b in HEK293 cells ectopically co-expressing both substrate and protease. However, no N-ICD formation was observed in the absence of SPPL2a or SPPL2b overexpression (Fig. 6, *A* and *B*). Based on the fact that ICDs are in general quite labile, we sought to stabilize N-ICD in HEK293 cells endogenously expressing SPPL2a/b and SPPL3. Upon treatment with bafilomycin A1, a low molecular weight V5-positive peptide was detected (Fig. 7*C*). Generation of this peptide was inhibited by simultaneous treatment with $(Z\text{-}LL)_2$ ketone and bafilomycin A1 (Fig. 7*C*). Together with the finding that overexpressed SPP and SPPL3 failed to generate N-ICD (Fig. 7, *A* and *B*), this

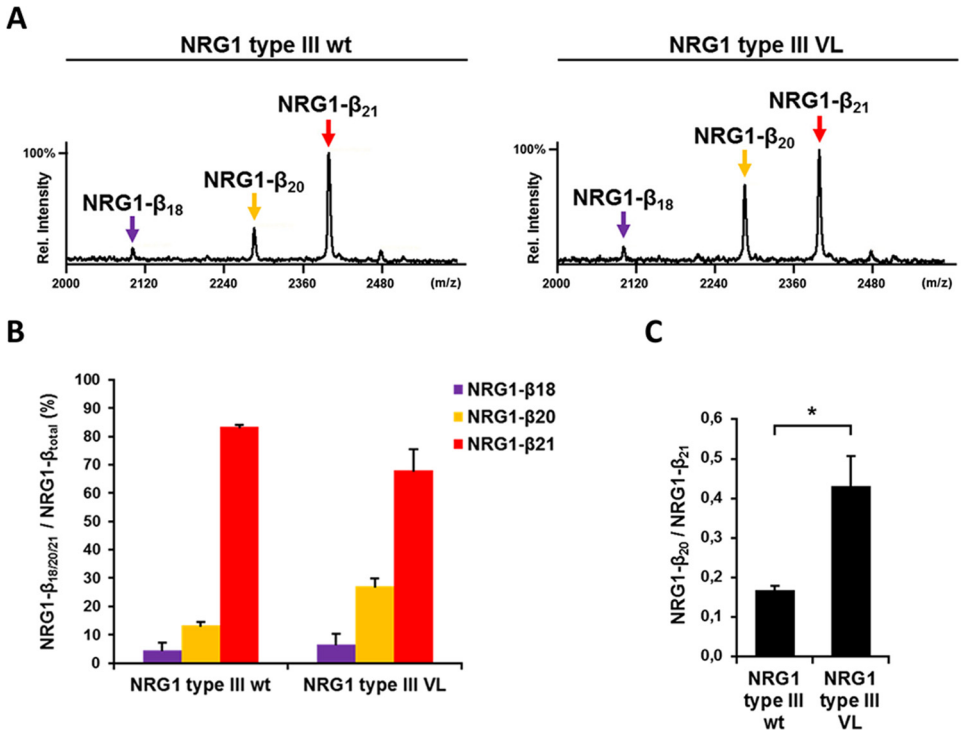

FIGURE 6. **Schizophrenia-associated valine to leucine mutation affects cleavage precision at the γ-site.** *A*, γ-secretase cleavage of NRG1 type III after Ala-313 is increased by the valine to leucine mutation. Supernatants of HEK293 cells transfected with BACE1 and wild-type (*wt*) or mutant (*VL*) NRG1 type III were immunoprecipitated with antibody 10E8, and isolated peptides were analyzed using MALDI-TOF mass spectrometry. In supernatants from cells expressing wild-type NRG1 type III, one major (NRG1-β21; *red arrow*) and two minor (NRG1-β20 and -β18; *yellow* and *purple arrow*) peptides were observed that are generated by γ-secretase cleavages after Leu-314, Ala-313, and Cys-311, respectively (see also Fig. 1, *C* and *D*). Compared with wild type, the valine to leucine mutation in NRG1 type III causes an increase in γ-secretase cleavage after Ala-313 (*yellow arrow*) leading to a higher intensity of the NRG1-β20 peak in the mass spectrum. *B* and *C*, semi-quantitative representation of the NRG1-β profile in *A*. The amount of each individual NRG1-β in the supernatant was determined by normalizing the area under the respective peak to the total peak area. Cells expressing the Val to Leu mutant of NRG1 type III release increased amounts of the shorter NRG1-β20 peptide, whereas the amount of the longer NRG1-β21 peptide is decreased. Together this leads to a significant change in the ratio of NRG1-β20 to NRG1-β21. Quantification from four independent experiments: mean ± S.D., *, $p < 0.05$, two-tailed unpaired Student's *t* test.

suggests that N-ICD production is mediated by endogenous SPPL2a/b (see also Fig. 8*C*).

C-peptide Is Generated by Endogenous SPPL2a and SPPL2b—Typically, SPPL2a- or SPPL2b-mediated intramembrane proteolysis leads to the generation of two characteristic cleavage products, an N-terminal intracellular ICD and a secreted C-peptide (13). To detect the latter cleavage product in cells expressing endogenous SPP/SPPLs, we generated a truncated NRG1 type III construct that comprises amino acids 2–114 and bears an N-terminal FLAG and a C-terminal V5 tag to detect products (FNRG-NTF-V5, Fig. 8*A*). We readily detected expression of FNRG-NTF-V5 in lysates of transiently transfected HEK293 cells (Fig. 8*B*). When conditioned media of these cells were subjected to α-V5 immunoprecipitation, we observed secretion of an ~5-kDa C-peptide, which was absent in supernatants of untransfected cells. Importantly, treatment of cells with $(Z\text{-}LL)_2$ ketone blocked secretion of the C-peptide and led to the accumulation of its precursor (Fig. 8*B*). To further confirm that endogenous SPPL2a and SPPL2b produce the C-peptide, we reduced expression of these proteases using RNAi. Western blot analysis confirmed efficient knockdown of SPPL2a and SPPL3 (Fig. 8*C*). Note that upon SPPL3 knockdown, SPPL2a is hyperglycosylated (Fig. 8*C*), which is in line with previous findings (19). Efficient knockdown of SPPL2b was confirmed by mRNA analysis (Fig. 8*C*, *lower panel*) due to the lack of an antibody detecting endogenous SPPL2b. Knockdown of SPPL2a and SPPL2b abolished C-peptide generation, whereas knockdown of SPPL3 still allowed normal C-peptide generation (Fig. 8, *C* and *D*) demonstrating that indeed endogenous SPPL2a/b activity mediates the C-peptide release.

Identification of the Intramembrane Cleavage Sites of the NRG1 Type III NTF′—To unambiguously demonstrate that NRG1 type III is subject to endoproteolysis within its N-terminal TMD, we determined the SPPL2a/SPPL2b cleavage site(s) in NRG1 type III by MALDI-TOF MS. We previously utilized truncated substrate constructs that include an N-terminal V5 and a C-terminal FLAG epitope tag to determine SPP/SPPL cleavage sites and have also included an alanine-proline motif at the very C terminus to prevent degradation by carboxypeptidases (19). We now generated a similar NRG1 type III (amino acids 2–114)-derived construct (V5-IIINRG-NTF-FLAG) and expressed this in HEK293 cells. FLAG-tagged C-peptides were purified from conditioned supernatants of transiently transfected cells and subjected to MALDI-TOF MS (Fig. 9, *A* and *B*). In DMSO-treated HEK293 cells, we detected one highly abundant and three less abundant NRG1 type III-derived peptides. The highly abundant peptide was generated by proteolytic cleavage following cysteine 92 of NRG1 type III, a site embedded within the predicted N-terminal TMD (Fig. 9, *B* and *C*). Two of the minor cleavage products likewise originate from proteolysis within the predicted TMD (cleavage after alanine 94 and glycine 95, respectively), whereas a third minor peptide

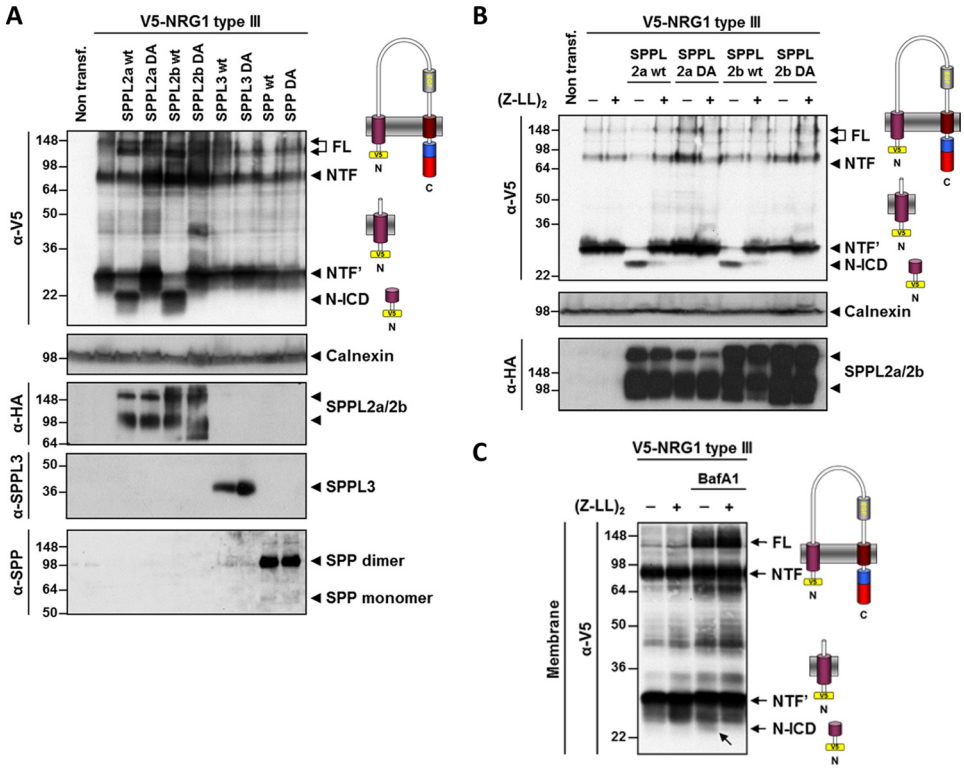

FIGURE 7. **NRG1 type III is a substrate for intramembrane proteolysis by SPPL2a and SPPL2b.** *A,* C-terminally truncated NRG1 type III NTF′ is endoproteolyzed by SPPL2a and SPPL2b but not by SPP and SPPL3. HEK293 cells or HEK293 cells stably expressing HA tagged wild-type or catalytically inactive mutants (DA) of SPPL2a, SPPL2b, SPP, or SPPL3 were transiently transfected with N-terminally V5-tagged NRG1 type III (V5-NRG1 type III). Isolated membranes were subjected to Western blot analysis for protease expression control. Calnexin was used as a loading control. *B,* SPPL2a/2b-mediated N-ICD generation is blocked by $(Z\text{-}LL)_2$ ketone treatment. As described in *A,* N-ICD generation was monitored in cells co-expressing V5-NRG1 type III and wild-type or mutant (DA) SPPL2a/2b. Cells were treated overnight with 20 μM $(Z\text{-}LL)_2$ ketone or with DMSO as control. Note that N-ICD generation was blocked by inhibitor treatment. Calnexin was used as loading control. *C,* bafilomycin A1 (*BafA1*) treatment stabilizes N-ICD. Concomitant treatment with bafilomycin A1 and $(Z\text{-}LL)_2$ ketone prevents generation of N-ICD.

occurs at isoleucine 104, immediately adjacent to the predicted TMD. Importantly, all four cleavage products were not observed in supernatants from cells treated with $(Z\text{-}LL)_2$ ketone (Fig. 9*A*). Collectively, these data demonstrate that NRG1 type III is subjected to intramembrane proteolysis also within its N-terminal TMD.

Thus, NRG1 type III is the first membrane protein that is endoproteolyzed by three different I-CLiPs, namely γ-secretase, SPPL2a, and SPPL2b. Additionally, NRG1 type III also undergoes processing by multiple sheddases, including BACE1, ADAM10, ADAM17, and a further so far unknown sheddase.

Discussion

NRG1 type III is probably one of the membrane-bound protease substrates, which undergoes the most complicated processing by a multitude of intramembrane-cleaving proteases and sheddases (Fig. 1*A*). We now know that NRG1 type III is cleaved within its ectodomain by at least three different proteases. These include BACE1, ADAM10, and ADAM17 (22–24). Apparently, BACE1 and to a lesser extent ADAM10 and -17 "open" up the loop to allow exposure of the EGF-like domain for ErbB3 signaling. Knock-out of BACE1 therefore reduces NRG1 signaling leading to a hypomyelination phenotype (22–24). ADAM10 and -17 can partially compensate explaining why the BACE1 knock-out does not cause a total demyelination phenotype. However, in addition BACE1, and also to some extent ADAM17, can perform a second cut, which then liberates the EGF-like domain to allow paracrine signaling (Fig. 1*A*) (24). Moreover, the remaining NTF is apparently further trimmed by a so far unknown sheddase, which generates the 28-kDa NTF′ in Figs. 1*A* and 7*A*. Thus, this is the first example of a regulated intramembrane proteolysis substrate, which requires dual shedding to allow subsequent cleavage by I-CLiPs. Both membrane-retained stubs are subject to intramembrane proteolysis. The CTF is cleaved by γ-secretase and generates an ICD as described before (26, 27). The physiological importance of BACE1-mediated NRG1 type III shedding (22–24) prompted us to investigate the subsequent generation of NRG1-β by γ-secretase. However, as NRG1 type III may also be shed by ADAMs, we assume that, in analogy to the processing of APP into Aβ and p3 peptides (51), γ-secretase cleavage of NRG1 type III also liberates a p3-like peptide by utilizing the same intramembrane cleavage sites. In that regard, we now also describe the production of NRG1-β, which is released into the extracellular space. Mass spectrometric analysis allowed us to determine the cleavage sites for the generation of both the NRG1 type III ICD and the NRG1-β peptide. The cleavage, which liberates the ICD, occurs after cysteine 321 and is located only five amino acids N-terminal to the membrane anchor of the second TMD. This fits well with previously identified ε-cleavage sites for other γ-secretase substrates (Fig.

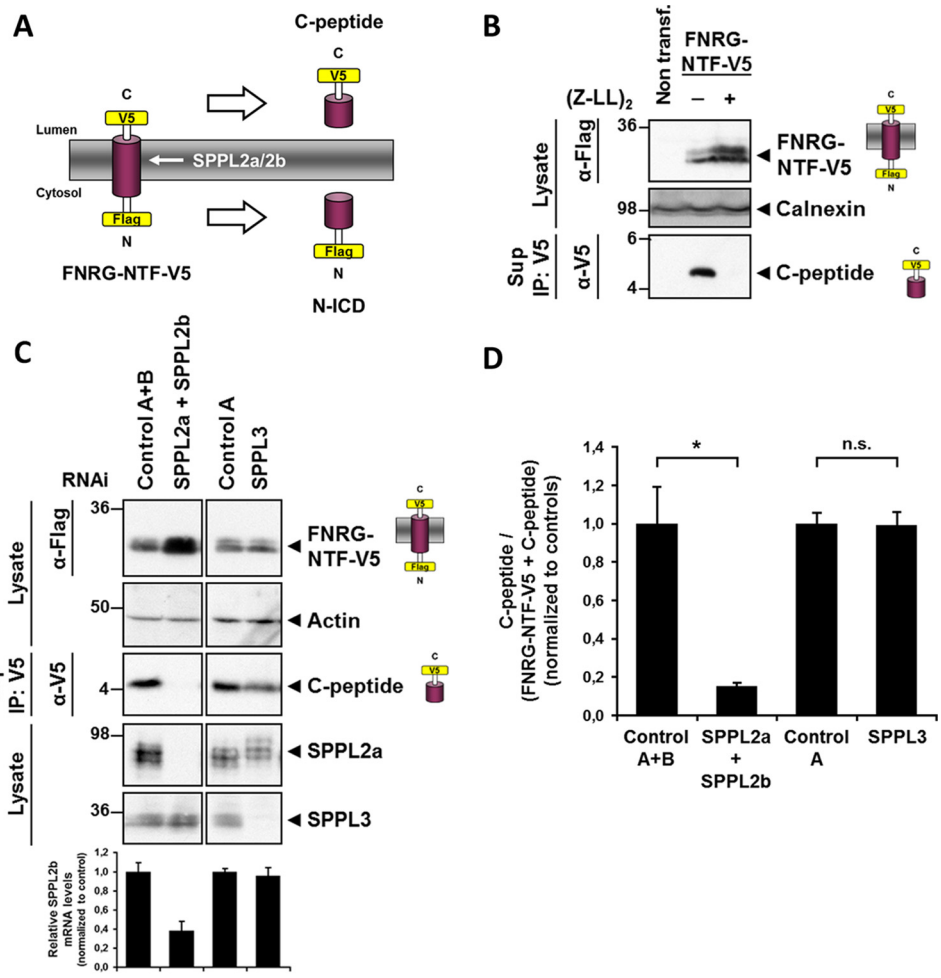

FIGURE 8. **C-peptide generation by SPPL2a/2b.** *A,* schematic overview of the truncated NRG1 type III construct used to analyze the SPPL2a/2b-mediated intramembrane proteolysis. Intramembrane proteolysis by SPPL2a/2b generates a secreted V5 tagged C-peptide and an N-terminal FLAG-tagged N-ICD. *B,* FNRG-NTF-V5 is cleaved by a $(Z\text{-}LL)_2$ ketone-sensitive endogenous protease activity in HEK293 cells. FNRG-NTF-V5 was transiently transfected into HEK293 cells. 24 h after transfection, cells were treated overnight with 20 μM $(Z\text{-}LL)_2$ ketone or DMSO, and conditioned supernatants were collected and subjected to anti-V5 immunoprecipitation to detect secreted C-peptides. Levels of full-length FNRG-NTF-V5 were examined in whole cell lysates, and calnexin was used as loading control. Note that inhibitor treatment blocks C-peptide secretion entirely and FNRG-NTF-V5 accumulates concomitantly. *C* and *D,* knockdown of SPPL2a/b but not SPPL3 abolishes C-peptide generation. Western blot and mRNA analysis confirms efficient knockdown of SPPL2a/b and SPPL3 (*lower panel*). Note that upon SPPL3 knockdown SPPL2a is hyperglycosylated (*C*) in line with previous findings (19). Quantification from three independent experiments: mean ± S.D., *, $p < 0.05$, two-tailed unpaired Student's *t* test.

10) (52). Moreover, the cleavage site is exactly at the peptide bond Cys-321/Val-322, just one amino acid N-terminal to the schizophrenia-associated V322L mutation (28). Consistent with previous findings, this mutation affects the turnover of the CTF (29), which may even be responsible for schizophrenia-like phenotypes in BACE1$^{-/-}$ mice (30). In addition, we now show that this mutation directly affects the turnover by γ-secretase, because the valine to leucine substitution significantly reduces not only the production of NRG1-β but also γ-secretase-dependent reverse signaling. One may thus speculate that either substrate accumulation due to reduced degradation by γ-secretase, cell autonomous reverse signaling via the ICD, or cell non-autonomous signaling via NRG1-β may be involved in schizophrenia-associated pathogenesis. Furthermore, similar to several familial Alzheimer disease-associated APP mutations, which occur within the C-terminal end of the APP TMD (49), the valine to leucine mutation shifts the cleavage at the γ-site. The cleavage site of NRG1-β is located after leucine 314 right within the middle of the TMD. This is consistent with the stepwise intramembrane proteolysis of other γ-secretase substrates (Fig. 10), which begins at the ε-cleavage site close to the C-terminal end of the TMD (53), followed by the ζ-cleavage, and finally terminates with the γ-cleavage (8, 9). These cleavages are spaced by roughly three amino acids, which may indicate proteolytic cleavages always after one helical turn. Liberation of the NRG1 ICD may allow further reverse signaling (26, 27). However, for the NRG1-β released on the other side of the membrane, no biological function is known. In fact, for Aβ and all other known β-like peptides, the physiological role is not clear. We therefore rather speculate that the additional ζ- and γ-cleavages may be required to fully remove the membrane stub after initiation of the signaling process by the liberation of the ICD. However, even the latter may not always be involved in reverse signaling. Although for the APP-ICD a signaling role has been suggested (54), its function and relevance are still unclear. The lack of a nuclear localization signal, a DNA bind-

A

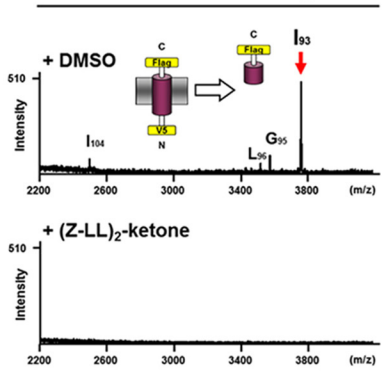

B

	Peptide	Cleavage after	Sequence	Mass [M+H]⁺ (Da) Calc.	Obs.
Major peptide	NRG1 type III C-peptide-I93	C92	I93AGLKWVFVDKIFEYDSPTHLD*DYKDDDDK*AP	3757.1	3762.6
Minor peptides	NRG1 type III C-peptide-G95	A94	G95LKWVFVDKIFEYDSPTHLD*DYKDDDDK*AP	3572.9	3578.0
	NRG1 type III C-peptide-L96	G95	L96KWVFVDKIFEYDSPTHLD*DYKDDDDK*AP	3515.8	3520.9
	NRG1 type III C-peptide-I104	K103	I104FEYDSPTHLD*DYKDDDDK*AP	2499.6	2503.4

C

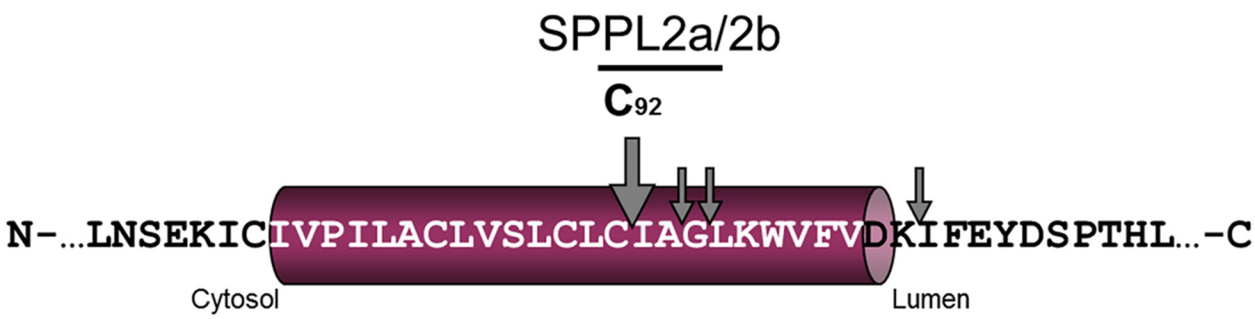

FIGURE 9. **Identification of the intramembranous cleavage sites of SPPL2a and -b.** *A,* to isolate C-peptides for mass spectrometric analysis, epitope tags of the truncated (amino acids 2–114) NRG1 type III construct described in Fig. 8 were inverted, and an alanine-proline motif was added to the FLAG tag at the C terminus to prevent degradation of C-peptides by carboxypeptidase activity. The resulting V5-IIINRG-NTF-FLAG was transfected into HEK293 cells, and cells were treated as described in Fig. 8. Conditioned supernatants were subjected to anti-FLAG IP, and immunoprecipitates were analyzed by MALDI-TOF mass spectrometry. One major (*red arrow*) and three minor peaks corresponding to V5-IIINRG-NTF-FLAG-derived peptides were observed in cells treated with DMSO but not upon $(Z\text{-}LL)_2$ ketone treatment. *B,* list of identified peptides and comparison of observed peptide mass to calculated mass. *Italic letters* indicate the FLAG tag, $[M + H]^+$ a singly charged peptide. *C,* schematic overview of the SPPL2a/2b cleavage sites within the N-terminal TMD of NRG1 type III. The N-terminal TMD (*magenta*) and flanking stretches are shown, and the $(Z\text{-}LL)_2$ ketone-sensitive cleavages are indicated by *gray arrows*.

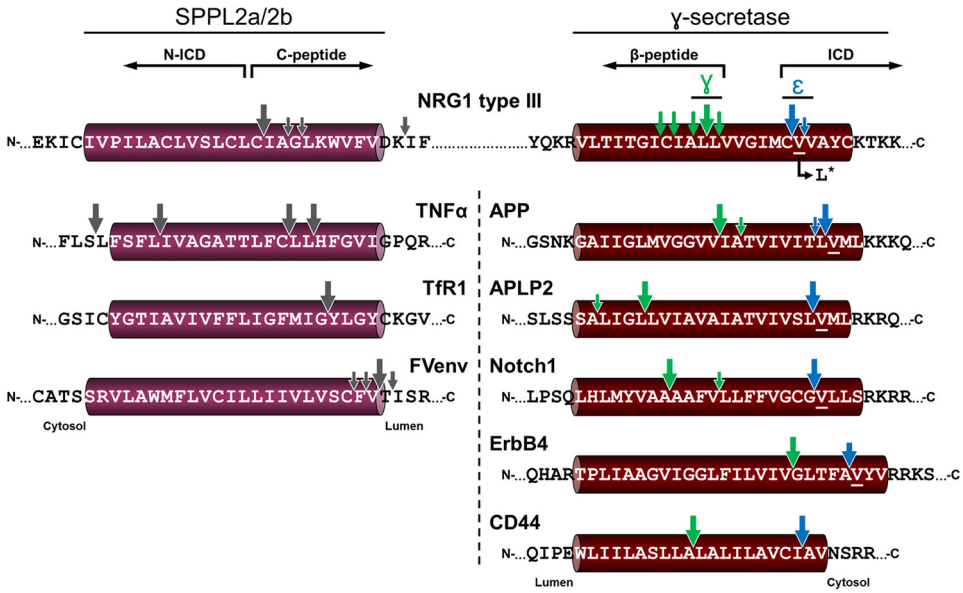

FIGURE 10. **Comparison of the intramembrane cleavage sites of γ-secretase and SPPL2a/2b substrates.** The sequences of SPPL2a/2b and γ-secretase substrates are shown on the *left* and *right*, respectively, and TMDs are indicated. Major cleavage sites are marked by *big arrows,* and *smaller arrows* denote the most frequent minor cleavage sites. Multiple less prominent sites in several substrates were omitted for clarity. The γ- and ϵ-like cleavage sites of the γ-secretase are indicated by *green* and *blue arrows*, respectively. A partially conserved valine residue at the P1′ position of the ϵ-like cleavage site is *underlined*. *Asterisk* denotes the schizophrenia-associated mutation in the TMD of NRG1 that affects cleavage by γ-secretase. The indicated cleavage sites are as follows: TNFα (16); TfR1 (36); foamy virus envelope protein (*FVenv*) (M. Voss, A. Fukumori, H. Steiner, C. Haass, and R. Fluhrer, unpublished data); APP (53, 58); APLP2 (59); Notch1 (46, 60, 61); ErbB4 (62–64); CD44 (65, 66); and NRG1 (28, 29).

ing domain, or a transcriptional activator domain rather suggests that the APP CTF may undergo complete degradation via the triple intramembrane cleavage (12).

The C-terminally truncated NTF′ of NRG1 type III also undergoes intramembrane cleavage, in this case by SPPL2a and SPPL2b, most likely in the lysosomal/late endosomal compartment. This fits well with the strict preference of proteases of the SPP and SPPL family for type 2-oriented membrane proteins (55–57). Moreover, this makes NRG1 type III besides tumor necrosis factor α (TNFα) (16, 17), transferrin receptor 1 (TfR1) (36), Bri2 (Itm2b) (34), the Foamy virus envelope protein (FVenv) (35), and the Fas ligand (18) another substrate of the SPPL2 subfamily. Similarly to the γ-cleavage of γ-secretase substrates, the NRG1 C-peptide is released by a cleavage within the mid-region of the TMD. However, in the case of SPPL2 substrates, this cleavage does not necessarily occur within the mid-region of the TMD but can rather be located between 0 and 9 amino acids away from the C-terminal end of the TMD (Fig. 10). Moreover, SPPL3 has recently been shown to liberate its substrates via a cleavage close to or just at the border of the TMD (19, 35). This may have rather interesting implications for differential substrate requirements and substrate recognition mechanisms for SPP/SPPL proteases and γ-secretase where the cleavage sites appear to be rather conserved (13, 56) As is the case for γ-secretase cleavage of the CTF, SPPL2a/2b releases a small peptide (C-peptide) into the extracellular space. Again, one may speculate about the function of the C-peptide and the ICD. Based on the lack of any functional domain within the N-ICD, we rather speculate that this cleavage may contribute to the final degradation of the NTF.

Taken together, NRG1 type III is the first regulated intramembrane proteolysis substrate, which undergoes shedding by at least three sheddases as well as intramembrane proteolysis by three different I-CLiPs. Furthermore, a schizophrenia-associated mutation is located only one amino acid C-terminal to the ϵ-cleavage site, and it not only reduces γ-secretase-dependent turnover of the CTF but also affects cleavage precision similar to some APP mutations.

Author Contributions—C. H. and M. W. designed the project, interpreted the data, and wrote the manuscript with the help of D. F. and M. V.; D. F. investigated γ-secretase-mediated processing; M. V. and R. F. investigated SPP/SPPL-mediated processing; B. B. and M. R. conducted the luciferase assay; C. G., H. H., and M. H.-K. provided technical support; B. S. and D. E. conducted the experiments in primary neurons; A. F. and H. S. helped with the mass spectrometry; E. K. generated monoclonal antibodies.

Acknowledgment—We thank Dr. Frauke van Bebber for critically reading this manuscript.

References

1. Brown, M. S., Ye, J., Rawson, R. B., and Goldstein, J. L. (2000) Regulated intramembrane proteolysis: a control mechanism conserved from bacteria to humans. *Cell* **100,** 391–398
2. Wolfe, M. S. (2009) Intramembrane-cleaving proteases. *J. Biol. Chem.* **284,** 13969–13973
3. Lichtenthaler, S. F., Haass, C., and Steiner, H. (2011) Regulated intramembrane proteolysis–lessons from amyloid precursor protein processing. *J. Neurochem.* **117,** 779–796
4. Haass, C., and Steiner, H. (2002) Alzheimer disease γ-secretase: a complex story of GxGD-type presenilin proteases. *Trends Cell Biol.* **12,** 556–562
5. Steiner, H., Kostka, M., Romig, H., Basset, G., Pesold, B., Hardy, J., Capell, A., Meyn, L., Grim, M. L., Baumeister, R., Fechteler, K., and Haass, C. (2000) Glycine 384 is required for presenilin-1 function and is conserved in bacterial polytopic aspartyl proteases. *Nat. Cell Biol.* **2,** 848–851
6. Haass, C. (2004) Take five–BACE and the γ-secretase quartet conduct Alzheimer's amyloid β-peptide generation. *EMBO J.* **23,** 483–488
7. Edbauer, D., Winkler, E., Regula, J. T., Pesold, B., Steiner, H., and Haass, C. (2003) Reconstitution of γ-secretase activity. *Nat. Cell Biol.* **5,** 486–488
8. Takami, M., Nagashima, Y., Sano, Y., Ishihara, S., Morishima-Kawashima, M., Funamoto, S., and Ihara, Y. (2009) γ-Secretase: successive tripeptide and tetrapeptide release from the transmembrane domain of β-carboxyl terminal fragment. *J. Neurosci.* **29,** 13042–13052
9. Qi-Takahara, Y., Morishima-Kawashima, M., Tanimura, Y., Dolios, G., Hirotani, N., Horikoshi, Y., Kametani, F., Maeda, M., Saido, T. C., Wang, R., and Ihara, Y. (2005) Longer forms of amyloid β protein: implications for the mechanism of intramembrane cleavage by γ-secretase. *J. Neurosci.* **25,** 436–445
10. Steiner, H., Fluhrer, R., and Haass, C. (2008) Intramembrane proteolysis by γ-secretase. *J. Biol. Chem.* **283,** 29627–29631
11. Haapasalo, A., and Kovacs, D. M. (2011) The many substrates of presenilin/γ-secretase. *J. Alzheimers Dis.* **25,** 3–28
12. Kopan, R., and Ilagan, M. X. (2004) γ-Secretase: proteasome of the membrane? *Nat. Rev. Mol. Cell Biol.* **5,** 499–504
13. Voss, M., Schröder, B., and Fluhrer, R. (2013) Mechanism, specificity, and physiology of signal peptide peptidase (SPP) and SPP-like proteases. *Biochim. Biophys. Acta* **1828,** 2828–2839
14. Weihofen, A., Binns, K., Lemberg, M. K., Ashman, K., and Martoglio, B. (2002) Identification of signal peptide peptidase, a presenilin-type aspartic protease. *Science* **296,** 2215–2218
15. Boname, J. M., Bloor, S., Wandel, M. P., Nathan, J. A., Antrobus, R., Dingwell, K. S., Thurston, T. L., Smith, D. L., Smith, J. C., Randow, F., and Lehner, P. J. (2014) Cleavage by signal peptide peptidase is required for the degradation of selected tail-anchored proteins. *J. Cell Biol.* **205,** 847–862
16. Fluhrer, R., Grammer, G., Israel, L., Condron, M. M., Haffner, C., Friedmann, E., Böhland, C., Imhof, A., Martoglio, B., Teplow, D. B., and Haass, C. (2006) A γ-secretase-like intramembrane cleavage of TNFα by the GxGD aspartyl protease SPPL2b. *Nat. Cell Biol.* **8,** 894–896
17. Friedmann, E., Hauben, E., Maylandt, K., Schleeger, S., Vreugde, S., Lichtenthaler, S. F., Kuhn, P. H., Stauffer, D., Rovelli, G., and Martoglio, B. (2006) SPPL2a and SPPL2b promote intramembrane proteolysis of TNFα in activated dendritic cells to trigger IL-12 production. *Nat. Cell Biol.* **8,** 843–848
18. Kirkin, V., Cahuzac, N., Guardiola-Serrano, F., Huault, S., Lückerath, K., Friedmann, E., Novac, N., Wels, W. S., Martoglio, B., Hueber, A. O., and Zörnig, M. (2007) The Fas ligand intracellular domain is released by ADAM10 and SPPL2a cleavage in T-cells. *Cell Death Differ.* **14,** 1678–1687
19. Voss, M., Künzel, U., Higel, F., Kuhn, P. H., Colombo, A., Fukumori, A., Haug-Kröper, M., Klier, B., Grammer, G., Seidl, A., Schröder, B., Obst, R., Steiner, H., Lichtenthaler, S. F., Haass, C., and Fluhrer, R. (2014) Shedding of glycan-modifying enzymes by signal peptide peptidase-like 3 (SPPL3) regulates cellular *N*-glycosylation. *EMBO J.* **33,** 2890–2905
20. Kuhn, P. H., Koroniak, K., Hogl, S., Colombo, A., Zeitschel, U., Willem, M., Volbracht, C., Schepers, U., Imhof, A., Hoffmeister, A., Haass, C., Rossner, S., Bräse, S., and Lichtenthaler, S. F. (2012) Secretome protein enrichment identifies physiological BACE1 protease substrates in neurons. *EMBO J.* **31,** 3157–3168
21. Zhou, L., Barão, S., Laga, M., Bockstael, K., Borgers, M., Gijsen, H., Annaert, W., Moechars, D., Mercken, M., Gevaert, K., Gevaer, K., and De Strooper, B. (2012) The neural cell adhesion molecules L1 and CHL1 are cleaved by BACE1 protease *in vivo*. *J. Biol. Chem.* **287,** 25927–25940
22. Willem, M., Garratt, A. N., Novak, B., Citron, M., Kaufmann, S., Rittger, A., DeStrooper, B., Saftig, P., Birchmeier, C., and Haass, C. (2006) Control of peripheral nerve myelination by the β-secretase BACE1. *Science* **314,** 664–666

23. Hu, X., Hicks, C. W., He, W., Wong, P., Macklin, W. B., Trapp, B. D., and Yan, R. (2006) Bace1 modulates myelination in the central and peripheral nervous system. *Nat. Neurosci.* **9,** 1520–1525
24. Fleck, D., van Bebber, F., Colombo, A., Galante, C., Schwenk, B. M., Rabe, L., Hampel, H., Novak, B., Kremmer, E., Tahirovic, S., Edbauer, D., Lichtenthaler, S. F., Schmid, B., Willem, M., and Haass, C. (2013) Dual cleavage of neuregulin 1 type III by BACE1 and ADAM17 liberates its EGF-like domain and allows paracrine signaling. *J. Neurosci.* **33,** 7856–7869
25. Fleck, D., Garratt, A. N., Haass, C., and Willem, M. (2012) BACE1-dependent neuregulin processing: review. *Curr. Alzheimer Res.* **9,** 178–183
26. Bao, J., Lin, H., Ouyang, Y., Lei, D., Osman, A., Kim, T. W., Mei, L., Dai, P., Ohlemiller, K. K., and Ambron, R. T. (2004) Activity-dependent transcription regulation of PSD-95 by neuregulin-1 and Eos. *Nat. Neurosci.* **7,** 1250–1258
27. Bao, J., Wolpowitz, D., Role, L. W., and Talmage, D. A. (2003) Back signaling by the Nrg-1 intracellular domain. *J. Cell Biol.* **161,** 1133–1141
28. Walss-Bass, C., Raventos, H., Montero, A. P., Armas, R., Dassori, A., Contreras, S., Liu, W., Medina, R., Levinson, D. F., Pereira, M., Leach, R. J., Almasy, L., and Escamilla, M. A. (2006) Association analyses of the neuregulin 1 gene with schizophrenia and manic psychosis in a Hispanic population. *Acta Psychiatr. Scand.* **113,** 314–321
29. Dejaegere, T., Serneels, L., Schäfer, M. K., Van Biervliet, J., Horré, K., Depboylu, C., Alvarez-Fischer, D., Herreman, A., Willem, M., Haass, C., Höglinger, G. U., D'Hooge, R., and De Strooper, B. (2008) Deficiency of Aph1B/C-γ-secretase disturbs Nrg1 cleavage and sensorimotor gating that can be reversed with antipsychotic treatment. *Proc. Natl. Acad. Sci. U.S.A.* **105,** 9775–9780
30. Savonenko, A. V., Melnikova, T., Laird, F. M., Stewart, K. A., Price, D. L., and Wong, P. C. (2008) Alteration of BACE1-dependent NRG1/ErbB4 signaling and schizophrenia-like phenotypes in BACE1-null mice. *Proc. Natl. Acad. Sci. U.S.A.* **105,** 5585–5590
31. Capell, A., Steiner, H., Willem, M., Kaiser, H., Meyer, C., Walter, J., Lammich, S., Multhaup, G., and Haass, C. (2000) Maturation and pro-peptide cleavage of β-secretase. *J. Biol. Chem.* **275,** 30849–30854
32. Steiner, H., Capell, A., Pesold, B., Citron, M., Kloetzel, P. M., Selkoe, D. J., Romig, H., Mendla, K., and Haass, C. (1998) Expression of Alzheimer's disease-associated presenilin-1 is controlled by proteolytic degradation and complex formation. *J. Biol. Chem.* **273,** 32322–32331
33. Steiner, H., Winkler, E., Shearman, M. S., Prywes, R., and Haass, C. (2001) Endoproteolysis of the ER stress transducer ATF6 in the presence of functionally inactive presenilins. *Neurobiol. Dis.* **8,** 717–722
34. Martin, L., Fluhrer, R., Reiss, K., Kremmer, E., Saftig, P., and Haass, C. (2008) Regulated intramembrane proteolysis of Bri2 (Itm2b) by ADAM10 and SPPL2a/SPPL2b. *J. Biol. Chem.* **283,** 1644–1652
35. Voss, M., Fukumori, A., Kuhn, P. H., Künzel, U., Klier, B., Grammer, G., Haug-Kröper, M., Kremmer, E., Lichtenthaler, S. F., Steiner, H., Schröder, B., Haass, C., and Fluhrer, R. (2012) Foamy virus envelope protein is a substrate for signal peptide peptidase-like 3 (SPPL3). *J. Biol. Chem.* **287,** 43401–43409
36. Zahn, C., Kaup, M., Fluhrer, R., and Fuchs, H. (2013) The transferrin receptor-1 membrane stub undergoes intramembrane proteolysis by signal peptide peptidase-like 2b. *FEBS J.* **280,** 1653–1663
37. Orozco, D., Tahirovic, S., Rentzsch, K., Schwenk, B. M., Haass, C., and Edbauer, D. (2012) Loss of fused in sarcoma (FUS) promotes pathological Tau splicing. *EMBO Rep.* **13,** 759–764
38. Fukumori, A., Okochi, M., Tagami, S., Jiang, J., Itoh, N., Nakayama, T., Yanagida, K., Ishizuka-Katsura, Y., Morihara, T., Kamino, K., Tanaka, T., Kudo, T., Tanii, H., Ikuta, A., Haass, C., and Takeda, M. (2006) Presenilin-dependent γ-secretase on plasma membrane and endosomes is functionally distinct. *Biochemistry* **45,** 4907–4914
39. Okochi, M., Steiner, H., Fukumori, A., Tanii, H., Tomita, T., Tanaka, T., Iwatsubo, T., Kudo, T., Takeda, M., and Haass, C. (2002) Presenilins mediate a dual intramembranous γ-secretase cleavage of Notch-1. *EMBO J.* **21,** 5408–5416
40. Walss-Bass, C., Liu, W., Lew, D. F., Villegas, R., Montero, P., Dassori, A., Leach, R. J., Almasy, L., Escamilla, M., and Raventos, H. (2006) A novel missense mutation in the transmembrane domain of neuregulin 1 is associated with schizophrenia. *Biol. Psychiatry* **60,** 548–553
41. Chen, Y., Hancock, M. L., Role, L. W., and Talmage, D. A. (2010) Intramembranous valine linked to schizophrenia is required for neuregulin 1 regulation of the morphological development of cortical neurons. *J. Neurosci.* **30,** 9199–9208
42. Brankatschk, B., Wichert, S. P., Johnson, S. D., Schaad, O., Rossner, M. J., and Gruenberg, J. (2012) Regulation of the EGF transcriptional response by endocytic sorting. *Sci. Signal.* **5,** ra21
43. Luo, X., Prior, M., He, W., Hu, X., Tang, X., Shen, W., Yadav, S., Kiryu-Seo, S., Miller, R., Trapp, B. D., and Yan, R. (2011) Cleavage of neuregulin-1 by BACE1 or ADAM10 protein produces differential effects on myelination. *J. Biol. Chem.* **286,** 23967–23974
44. Capell, A., Steiner, H., Romig, H., Keck, S., Baader, M., Grim, M. G., Baumeister, R., and Haass, C. (2000) Presenilin-1 differentially facilitates endoproteolysis of the β-amyloid precursor protein and Notch. *Nat. Cell Biol.* **2,** 205–211
45. Hu, X., He, W., Diaconu, C., Tang, X., Kidd, G. J., Macklin, W. B., Trapp, B. D., and Yan, R. (2008) Genetic deletion of BACE1 in mice affects remyelination of sciatic nerves. *FASEB J.* **22,** 2970–2980
46. Okochi, M., Fukumori, A., Jiang, J., Itoh, N., Kimura, R., Steiner, H., Haass, C., Tagami, S., and Takeda, M. (2006) Secretion of the Notch-1 Aβ-like peptide during Notch signaling. *J. Biol. Chem.* **281,** 7890–7898
47. Harrison, P. J., and Law, A. J. (2006) Neuregulin 1 and schizophrenia: genetics, gene expression, and neurobiology. *Biol. Psychiatry* **60,** 132–140
48. Mei, L., and Xiong, W. C. (2008) Neuregulin 1 in neural development, synaptic plasticity and schizophrenia. *Nat. Rev. Neurosci.* **9,** 437–452
49. Suzuki, N., Cheung, T. T., Cai, X. D., Odaka, A., Otvos, L., Jr., Eckman, C., Golde, T. E., and Younkin, S. G. (1994) An increased percentage of long amyloid β protein secreted by familial amyloid β protein precursor (β APP717) mutants. *Science* **264,** 1336–1340
50. Krawitz, P., Haffner, C., Fluhrer, R., Steiner, H., Schmid, B., and Haass, C. (2005) Differential localization and identification of a critical aspartate suggest non-redundant proteolytic functions of the presenilin homologues SPPL2b and SPPL3. *J. Biol. Chem.* **280,** 39515–39523
51. Haass, C., Hung, A. Y., Schlossmacher, M. G., Teplow, D. B., and Selkoe, D. J. (1993) β-Amyloid peptide and a 3-kDa fragment are derived by distinct cellular mechanisms. *J. Biol. Chem.* **268,** 3021–3024
52. Steiner, H., and Haass, C. (2000) Intramembrane proteolysis by presenilins. *Nature Rev. Mol. Cell Biol.* **1,** 217–224
53. Sastre, M., Steiner, H., Fuchs, K., Capell, A., Multhaup, G., Condron, M. M., Teplow, D. B., and Haass, C. (2001) Presenilin-dependent γ-secretase processing of β-amyloid precursor protein at a site corresponding to the S3 cleavage of Notch. *EMBO Rep.* **2,** 835–841
54. Cao, X., and Südhof, T. C. (2001) A transcriptionally [correction of transcriptively] active complex of APP with Fe65 and histone acetyltransferase Tip60. *Science* **293,** 115–120
55. Fluhrer, R., Steiner, H., and Haass, C. (2009) Intramembrane proteolysis by signal peptide peptidases: a comparative discussion of G*X*GD-type aspartyl proteases. *J. Biol. Chem.* **284,** 13975–13979
56. Lemberg, M. K., and Martoglio, B. (2002) Requirements for signal peptide peptidase-catalyzed intramembrane proteolysis. *Mol. Cell* **10,** 735–744
57. Martin, L., Fluhrer, R., and Haass, C. (2009) Substrate requirements for SPPL2b-dependent regulated intramembrane proteolysis. *J. Biol. Chem.* **284,** 5662–5670
58. Weidemann, A., Eggert, S., Reinhard, F. B., Vogel, M., Paliga, K., Baier, G., Masters, C. L., Beyreuther, K., and Evin, G. (2002) A novel ε-cleavage within the transmembrane domain of the Alzheimer amyloid precursor protein demonstrates homology with Notch processing. *Biochemistry* **41,** 2825–2835
59. Hogl, S., Kuhn, P. H., Colombo, A., and Lichtenthaler, S. F. (2011) Determination of the proteolytic cleavage sites of the amyloid precursor-like protein 2 by the proteases ADAM10, BACE1 and γ-secretase. *PLoS One* **6,** e21337
60. Huppert, S. S., Le, A., Schroeter, E. H., Mumm, J. S., Saxena, M. T., Milner, L. A., and Kopan, R. (2000) Embryonic lethality in mice homozygous for a processing-deficient allele of Notch1. *Nature* **405,** 966–970
61. Schroeter, E. H., Kisslinger, J. A., and Kopan, R. (1998) Notch-1 signalling requires ligand-induced proteolytic release of intracellular domain. *Nature* **393,** 382–386

62. Ni, C. Y., Murphy, M. P., Golde, T. E., and Carpenter, G. (2001) γ-Secretase cleavage and nuclear localization of ErbB-4 receptor tyrosine kinase. *Science* **294,** 2179–2181
63. Lee, H. J., Jung, K. M., Huang, Y. Z., Bennett, L. B., Lee, J. S., Mei, L., and Kim, T. W. (2002) Presenilin-dependent γ-secretase-like intramembrane cleavage of ErbB4. *J. Biol. Chem.* **277,** 6318–6323
64. Vidal, G. A., Naresh, A., Marrero, L., and Jones, F. E. (2005) Presenilin-dependent γ-secretase processing regulates multiple ERBB4/HER4 activities. *J. Biol. Chem.* **280,** 19777–19783
65. Okamoto, I., Kawano, Y., Murakami, D., Sasayama, T., Araki, N., Miki, T., Wong, A. J., and Saya, H. (2001) Proteolytic release of CD44 intracellular domain and its role in the CD44 signaling pathway. *J. Cell Biol.* **155,** 755–762
66. Lammich, S., Okochi, M., Takeda, M., Kaether, C., Capell, A., Zimmer, A. K., Edbauer, D., Walter, J., Steiner, H., and Haass, C. (2002) Presenilin-dependent intramembrane proteolysis of CD44 leads to the liberation of its intracellular domain and the secretion of an Aβ-like peptide. *J. Biol. Chem.* **277,** 44754–44759

Proteolytic Processing of Neuregulin 1 Type III by Three Intramembrane-cleaving Proteases

Daniel Fleck, Matthias Voss, Ben Brankatschk, Camilla Giudici, Heike Hampel, Benjamin Schwenk, Dieter Edbauer, Akio Fukumori, Harald Steiner, Elisabeth Kremmer, Martina Haug-Kröper, Moritz J. Rossner, Regina Fluhrer, Michael Willem and Christian Haass

J. Biol. Chem. 2016, 291:318-333.
doi: 10.1074/jbc.M115.697995 originally published online November 16, 2015
